Environmental Challenges 5 (2021) 100405

Contents lists available at ScienceDirect

Environmental Challenges

journal homepage: www.elsevier.com/locate/envc

Recent developments and application of bimetallic based materials in water purification

Bharat Kumar Allam [a,*], Neksumi Musa [b], Abhijit Debnath [c], Usman Lawal Usman [b], Sushmita Banerjee [b,*]

[a] Department of Chemistry, Rajiv Gandhi University, Rono Hills, Arunachal Pradesh, India
[b] Department of Environmental Sciences, Sharda University, Greater Noida, India
[c] Department of Civil Engineering, Indian Institute of Technology (BHU), Varanasi, India

ARTICLE INFO

Keywords:
Bimetal
Bimetal oxide
Heavy metals
Radionuclides
Pharmaceuticals
Wastewater

ABSTRACT

The shortage of clean drinking water is of great concern in many parts of the world. This problem results from a rapid population increase, defiling water resources, protracted droughts, and flooding due to climate change and anthropogenic activities. The scientific research that focuses on designing efficient materials to purify and recycle water is of paramount importance. Treatment of wastewater using traditional methods remain inefficient for providing sufficient, safe, and drinking water due to an increase in the water demand, coupled with the strict health guidelines for the level of contaminants in drinking water by the World Health Organization (WHO) and the United States Environmental Protection Agency (USEPA). Presently, highly efficient wastewater treatment is attainable due to the availability of affordable multifunctional nanomaterials. Bimetallic nanomaterials are designed by incorporating two dissimilar metals. These bimetallic materials exhibit more efficient characteristics than parental metal precursors due to the extensive array of chemical and physical properties, synergistic effects, and different mechanisms of action. This review highlights the recent developments in the synthesis and applications of bimetallic nanomaterials to remove various pollutants from water.

1. Introduction

Safe and adequate drinking water is necessary for the nourishment and survival of human beings. In 2010, the United Nations General Assembly (UNGA) stressed the importance of clean drinking water and sanitation and recognized them as a fundamental and essential part of human rights (Organization, 2019). The availability of clean drinking water is a critical index to determine development and well-being. The availability of adequate drinking water tremendously influences all aspects of life and accelerates society's socio-economic growth (Fry et al., 2016; Kanan et al., 2020; Schellenberg et al., 2020). By 2025, significant countries hit by water pollution and half of the earth's total population will live under water-stressed zones (Ahuja, 2021). Organic, inorganic and biological materials are released into the environment via human activities, intensely undermining the water quality (Scaria et al., 2020). Annually, approximately ten to twenty million people die because of improper water treatment (Organization, W.H., UNICEF. 2013). Six thousand children are dying daily because of the health complications associated with waterborne diarrhoea (Haller et al., 2007). However, conventional water treatment methods are less efficient to eliminate many of the toxic substances. The emerging research on the wastewater treatment stresses the need for sustainable, economical, and efficient water decontamination methods (Banerjee and Sharma, 2019). Conventional treatment methods like flocculation, coagulation, chlorination, ozonation, ultraviolet (UV), photolysis, ion exchange, reverse osmosis (RO), and ultra-filtration have limited efficacy in removing emerging pollutants (Gopal et al., 2007; Qin et al., 2007; Urase and Kikuta, 2005; Vieno et al., 2006; Walha et al., 2007). New innovative techniques and treatment procedures are essential to treat newly emerging micropollutants. among the different techniques of water remediation, the nanotechnology based methods are highly efficient and economical in achieving the safe drinking water (Li et al., 2016). Nanomaterials are sufficiently tackling several problems concerning the quality of water because of the attractive properties such as enhanced surface area, strong adsorption, superior redox properties, photocatalytic activity and easily tunable reactivity (Qu et al., 2013; Savage and Diallo, 2005).

Recently, bimetallic nanoparticles have gained significant attention from the research community due to their distinctive catalytic, electronic, optical, and magnetic properties (Li et al., 2020). Bimetallic nanoparticles are a specific category of materials comprised of two metals and display new capacities because of the synergistic effects (He et al., 2020; Sharma et al., 2019a).

* Corresponding author.
E-mail addresses: bharat.allam@rgu.ac.in (B.K. Allam), sushmita.banerjee@sharda.ac.in (S. Banerjee).

https://doi.org/10.1016/j.envc.2021.100405
Received 29 July 2021; Received in revised form 20 November 2021; Accepted 24 November 2021

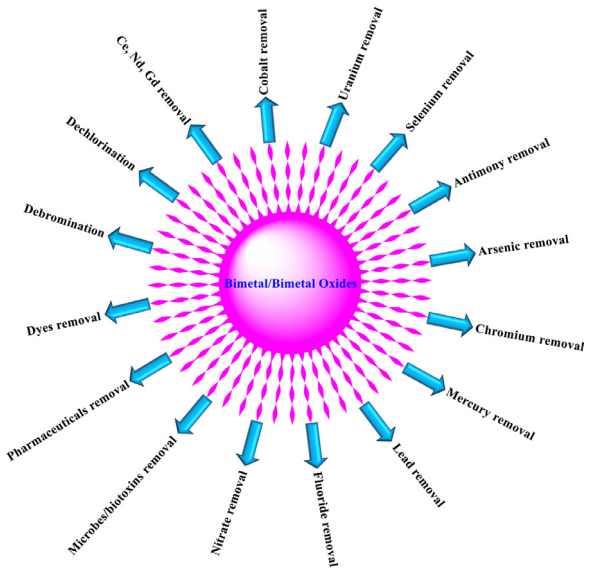

Fig. 1. Removal of various pollutants using bimetal/bimetal oxide.

In comparison to monometallic nanoparticles, bimetallic nanoparticles (nano alloys) exhibit a higher pollutant removal ability. Based on the structural features resulting from the fabrication method, these nanoparticles can be classified as multi-shell, core-shell segregated, intermetallic (alloyed), and heterogeneous structures (Ferrando and Jellinek, 2009). The variety of these nanostructures is mainly dependent on the nature of the combining metals, which is primarily determined by factors such as the relative bond strength, surface energy, atomic dimensions, transfer of charge, and specific electronic and magnetic effects (Liu et al., 2014).

This review discusses the recent development in the synthesis and application of bimetallic nanomaterials to remove toxic heavy metals, organic compounds, inorganic solutes, and microbes (Fig. 1).

2. Physio-chemical and biological methods of bimetal nanoparticles synthesis

Generally, the leading synthetic processes (Fig. 2) for the bimetallic nanoparticles are:

2.1. Physical methods

Physical methods include radiolysis, mechanical alloying, sonochemical and arc-discharge plasma techniques.

(a) Radiolysis method

The radiolysis method is a prolific method for the synthesis of bimetallic nanoparticles. This method generates solvated electrons by subjecting an aqueous solution containing stabilizer ligands and metal precursors to gamma irradiation. The metal ions could be converted to metal atoms through the acceptance of electrons by the metal ions. The new metallic atoms will then collectively combine into a bimetallic nanomaterial (Sankar et al., 2012). The intensity of the gamma radiation is a determining factor and decide the resultant type of the nano structure. A low dose can create core-shell bimetallic nanoparticles, whereas a higher dose controls the making of mixed bimetallic nanoparticles. Bimetals such as Ag–Pd, Ag–Pt, Au–Pt, and Pt–Ni can be prepared using this method (Mirdamadi-Esfahani et al., 2010; Yuan et al., 2020).

(b) Mechanical alloying method

Mechanical alloying is a convenient and efficient solid-state powder processing technique involving repeated cold welding and fracturing powder particles in a high energy ball mill (Taha et al., 2019). Bimetallic nanoparticles synthesized using this method are mostly used for dechlorination, hydrogenation, and hydrogen generation (Fu et al., 2015). Factors such as milling time, the concentration of additives, milling parameters, and phase composition significantly affect the products of this method. Bimetals of aluminium (Al–Bi and Al–Sn), Mg–Pd, Mg–Cd, and Ti–Fe nano-composites are synthesized using this method (Dębski et al., 2021; Gómez et al., 2020; Liang and Schulz, 2004; Liu et al., 2012).

(c) Sonochemical synthesis

Sonochemical synthesis is a valuable technique for the fabrication of bimetallic nanoparticles. The metal ions reduction can be achieved using ultrasound radiation. The nanocomposites of Fe–Co (20 kHz in organic solvent),(Dabala et al., 2008) Au–Pd (200 kHz in aqueous solution),(Mizukoshi et al., 2010) and Au–Ag (20 kHz in aqueous solution)(Anandan et al., 2008) are some of the bimetals synthesized using the sonochemical synthesis method.

(d) Arc-discharge plasma technique

In the electrical methods, the synthesis of the bimetallic nanoparticles is achieved through the generation of the plasma by the arc discharged from direct current (DC) or alternate current (AC) or pulsed current (PC). The Ag–Cu and Ni–Fe bimetal nanoparticles were synthesized using the arc-discharge plasma technique (Qu et al., 2020; Rahaghi et al., 2015).

2.2. Chemical methods

The chemical methods consist of reduction, seed growth, and diffusion.

(a) Chemical reduction

The chemical reduction could be either a simultaneous or successive reduction. Metal ions are produced from their respective metal precursors and subsequently reduced to metal atoms with the aid of a reductant, thereby causing an increase in the concentration of metal atoms. The high concentration of metal atoms usually results in supersaturation, nucleation, and growth (Ali et al., 2021). Due to the differences in the redox potential of metal precursors, the morphology of bimetals can be controlled using a co-reduction method. Nanoparticles in the zero-valent state are usually produced from the chemical reduction method (Sharma et al., 2019a). The metal with a high redox potential forms the core of a bimetallic nanoparticle, and the metal with a low reduction potential accumulates on the surface of the core metal. Owing to the difference in redox potentials and other chemical properties of the metal precursors, the nucleation and reduction procedure tends to be challenging to control in situations where more potent reducing agents are used (Quinson and Jensen, 2020). To surmount this inadequacy, the use of compatible surfactants or ligands that are polymeric make the particle's surface inactive or less reactive to gain control over the reduction process (Alexander et al., 2020). Au–Pt bimetallic nanoparticles were prepared successfully using the surfactant-assisted chemical reduction technique (Cao et al., 2013). Another way of controlling the reduction and nucleation process is by making usage of mild reductants (Vilardi et al., 2021). Bimetal nanocrystals of Au–Pd, Au–Rh, Au–Pt can be successfully prepared using a mild chemical reduction method (Han et al., 2015). The chemical reduction method to control crystal anisotropy polymer/TIPS pentacene can enhance uniformity and reduce crystal disorientation (He et al., 2011; Vilardi and Verdone, 2020).

(b) Seeding growth technique

The seeding growth technique is a reliable route to synthesize heterostructure and core-shell bimetal nanoparticles. The hetero structure can be fabricated via the deposition of a secondary metal on different and

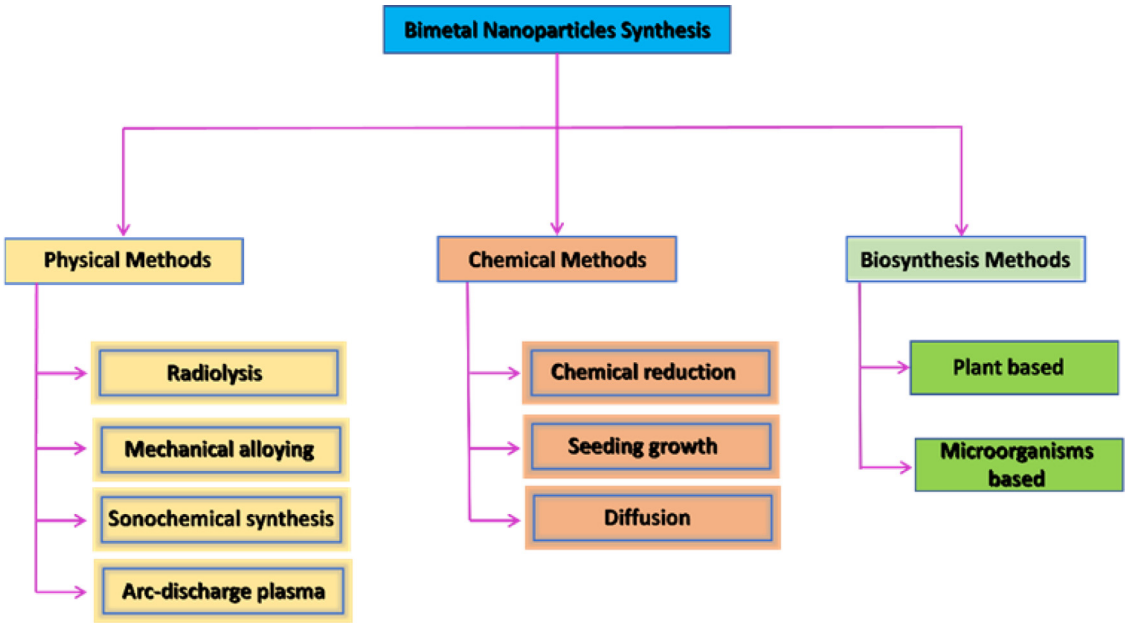

Fig. 2. Various methods for bimetal synthesis.

distinctive sites of the seed metal. A core-shell form can be produced by the deposition of a second metal on the surface of a seed metal (De Souza et al., 2019). The seeding growth method offers precision in the morphology and control over kinetic and thermodynamic variables. Bimetallic nanoparticles of Ag/Ru (Adekoya et al., 2014) and Au/Ag was synthesized using this method (Yu and He, 2015).

(c) Diffusion method

Diffusion is a mild and easy method to synthesize bimetals that possess a homogeneous structural morphology like the one found in core-shell bimetallic nanoparticles. The diffusion method offers many advantages over the chemical reduction method. The diffusion method was successfully employed to synthesise Au–Sn nanocrystals at room temperature (Zhang et al., 2012).

(d) Biosynthesis method

The biosynthesis method for synthesising bimetallic-based nanoparticles uses safe and environmentally friendly reducing agents such as extracts and powders of plants to achieve metal ions reduction. For the synthesis of bimetals using the biological method, two different mechanisms can be used. The first mechanism (Bio-reduction) can be achieved by biologically reducing the metal ions into stable forms. The second mechanism (bio sorption) is achieved by bonding of metal ions with organisms and subsequent conversion to their stable forms (Jiang et al., 2019). The functional groups on the reducing agents serve as crucial components in the bimetals reduction and capping. This whole process is usually conducted at room temperature. It is typically applied in synthesising Au-Ag bimetallic nanoparticles (Using fruit juice of pomegranate/ mahogany leaf extract/ Anacardium occidentale leaf powder). The phenolic polyhydroxy compounds and proteins present in these plant extracts and powders are responsible for the bio reduction.

3. Common synthetic methods for bimetallic oxides

The typical synthesis methods for the bimetallic oxides are spray pyrolysis, precipitation, hydrothermal, sol-gel and impregnation methods (Fig. 3). The factors such as calcination temperature, depositional path, the choice and proportion of chemical precursors, and the solvent's composition generally affect the performance and properties of the synthesized bimetallic oxides.

3.1. Spray pyrolysis

Spray pyrolysis is an efficient, reproducible, and low-cost method for synthesizing thin films and nano-powders of bimetal oxides from their metal precursor solutions. The metal precursor solutions are atomized into tiny uniform droplets. These droplets are subjected to rapid heating, controlled thermolysis, and inert gas flow to result in thin films of the bimetal oxides. The Y–Fe, Mg–Al and Mn–Zn oxide thin films were prepared using spray pyrolysis (Todorovska et al., 2002) (Rocheleau et al., 1994) (Mansour et al., 2020). The bimetal oxide nano-powders can be prepared by subjecting the metal precursor gels to slowly burning at an elevated temperature. Ashes resulting from the smouldering process are ground to an ultrafine powder form (Jung et al., 2010).

3.2. Precipitation method

The precipitation method is a wet chemical method for the synthesis of non-crystalline nano bimetal oxides. Ammonia and sodium hydroxide were used as precipitating agents (Vilardi, 2020) (Chai et al., 2013). Keeping an optimum temperature for the calcination followed by a careful sediment partition controls the nano particle size. The addition of stabilizing agents and dispersants eliminate the agglomeration. The bimetal oxides of Fe–Mn, Ni–Mn and Fe–Ti were synthesized using the precipitation method (Chen et al., 2012; Eslami et al., 2019; Wan et al., 2014).

3.3. Hydrothermal method

The hydrothermal synthesis produces high purity bimetallic oxides. This method exposes the metal precursors to forced hydrolysis by placing them in an autoclave at moderate temperature and high pressure. This system can synthesize bimetal oxides having porous structural morphologies (Wangcheng et al., 2014). The structure of the bimetal oxide can be altered by changing metal precursors composition, pH of the solvent, reaction time, and autoclave temperature (Ocsoy et al., 2017). Using hydrothermal method, Bi–Nb, Cu–Co, Sb–Mo oxides were synthesized and applied in various applications (Alcântara et al., 2018; Sun et al., 2021; Wang et al., 2019).

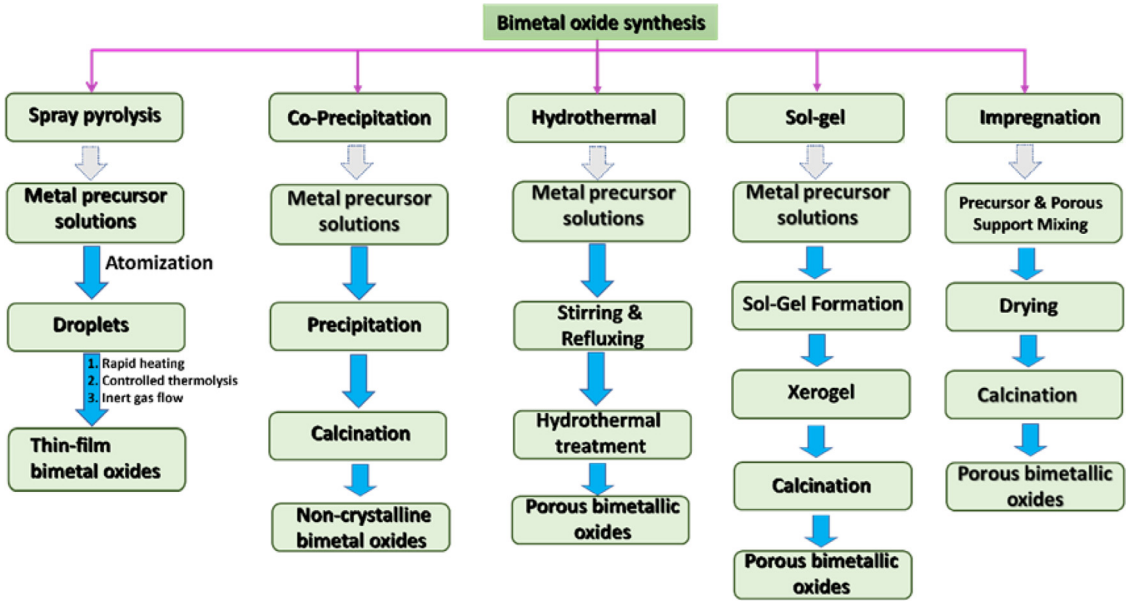

Fig. 3. Different techniques for bimetal oxide synthesis.

3.4. Sol-gel method

The sol-gel method involves a solution transformed into a gel and then deposited on a surface (Vilardi et al., 2019b). The bimetallic oxides with either mesoporous or microporous morphology are synthesized by the initial hydrolysis of the metal precursors followed by polymerizers to polymerize the metal precursors, resulting in the formation of a sol-gel (Darmawan et al., 2017). It is possible to have bimetallic oxides with different structures due to varying factors such as calcination temperatures, sol-gel procedural difference, and templates' concentration (Polat et al., 2015). The bimetal oxides of Zn–Fe, Co–Cu, and La–Fe were synthesized using the sol-gel method (Feng et al., 2011; Luo et al., 2019; Veith et al., 2005).

3.5. Impregnation method

The impregnation method offers the simplest way for the synthesis of bimetallic oxides. An aqueous solution of the metal precursor is impregnated into an initially prepared metal oxide support and subjected to calcination. In a "wet" impregnation process, an excess amount of the solution of the metal precursor is used to prepare a thin slurry, and in the dry impregnation process, a limited amount of the metal precursor solution is used to fill the pore volume of the support (Mehrabadi et al., 2017). The bimetal oxides of Mg–Fe, V–Cu, and Fe–Ni can be prepared using the impregnation method (Tao et al., 2013; Li et al., 2021a; Park et al., 2021).

4. Remediation of pollutants removal using bimetals and bimetal oxides

The utilization of bimetal and bimetal oxides to remove various pollutants from wastewater is currently gained significant attention from researcher across the globe. The choice of the metal combination and synthesis technique controls the efficacy of the pollutant removal process. Moreover, the fine tuning of the process parameters such as adsorbent/catalyst dose, temperature, solution pH, contact time, and interfering anions is important for achieving optimal sorbent performance (Table 1).

4.1. Heavy metals removal

Toxic heavy metal pollution of the environment is becoming a severe problem of the world. The typical heavy metal ions are Pb(II), Cr(VI), Mn(II), Ni(II), As(V), Cd(II), Hg(II) etc. These inorganic pollutants readily enter the soil, water, and atmosphere due to the rapid industrialization, mining activities, improper waste disposal, the use of heavy metal pesticides and fertilizers, and the chemical weathering of heavy metal enriched rocks and minerals. Heavy metals are nonbiodegradable and induce carcinogenic effects in human beings (Parvin et al., 2019).

Heavy metal removal is highly required to supply pure water and to maintain ecological balance. Nanomaterials serve as efficient adsorbents in the decontamination of heavy metals due to their excellent surface to volume ratio, availability of more active sites for binding, high removal efficiencies and easy reusability. among the nanomaterials, bimetal and bimetallic nanomaterials are highly effective in removing heavy metals due to their highly selective adsorption capacity (Wadhawan et al., 2020).

(a) Use of bimetals for heavy metals removal

Redox reactions, dissolution, precipitation, desorption, and adsorption influence the transformation, mobility, and solubility of heavy metals, consequently determining the toxicity of heavy metals in the environment (Fu and Wang, 2011). Bimetals have shown tremendous redox activity concerning the removal of heavy metal ions through their adsorption capacity, as revealed by recent research in water remediation (Song et al., 2021). Iron-based bimetallic nanoparticles are a common adsorbent used for the removal of heavy metals. The metal removal efficiency was enhanced by tailoring the surface-active sites. The use of bimetals comprises palladium/silver/nickel/zirconium and zero-valent iron (Ali et al., 2021). The removal of cadmium, arsenic, chromium, and mercury from water by using bimetallic iron (Fe) based nanoparticles has so far encountered great success. The Fe–Ni nanoparticles were used for the As(V) removal from mining waste water. The calcinated Fe–Ni bimetal was synthesized using eucalyptus leaf extract as a reducing agent. The adsorption process followed a spontaneous endothermic pathway and best fit the Langmuir isotherm model. The kinetics of the method followed a pseudo-second order rate model, and the removal efficiency was observed as 82.6%. The electrostatic interaction found to play a significant role in the arsenic removal process (Lin et al., 2022) (Fig. 4).

Table 1
Bimetal/bimetal oxide mediated pollutant removal methods.

Bimetal/ Bimetal oxides	Pollutant	Dosage of catalyst & initial conc. of pollutants	Removal Efficiency	Optimum pH	Research Highlights	Reference
TiO_2/ nZVI	Nitrate	0.982 g/L for 200 mg/L of NO_3^- conc. (TiO_2:nZVI 7:1)	98.226% within 150.091 min	4.1	Grafting of TiO_2 into nZVI reduces agglomeration behaviour of Fe^0 improves removal efficiency.	(Hejri et al., 2019)
Pd–Sn/γ–Al_2O_3–diatomite	Nitrate	3 g/L (Pd:Sn 3:1) 2:1 of γ–Al_2O_3: diatomite (for 0.04 to 0.24 mg/L of NO_2^- conc.)	Catalytic activity 0.42 mg/L·g·min; N_2 selectivity 70%	5.2	High surface area and good porosity of the composite facilitates rapid transfer of electron thus enhances catalytic activity.	(Hao and Zhang, 2017)
MgO/Fe_3O_4 embedded activated carbon	Malachite Green	0.2 g/L for 500 & 800 mg/L of MG	99% for 500 mg/L of MG within 360 min	> 6	Hydrogen bonding, π–π stacking and electrostatic attraction plays important role in the sorption process. Contribution of Nitrogen group from MG dye bind actively with OH group of adsorbents.	(Guo et al., 2020)
Kaolin-supported bimetallic Fe/Ni	Direct Black G	2.1 g/L for 50–800 mg/L of DBG	99.97% within 40 min for 50 mg/L of DBG at 313 K	3.0	Fe corrosion followed by H^+ ion transfer to form nickel hydride which further promotes azo bond cleavage.	(Liu et al., 2013b)
Ni–Fe	Trichloroethylene, TCE	Ni–Fe (Ni content (2 wt.%); 3.3 g/L for initial TCE conc. 50 mg/L	90% in 90 min of reaction time	8.1–8.3	Ni–Fe offers high electrochemically stable surface sites and possess good chemical resistance to Cl^-, HCO_3^-, & organic matter while PO_4^{3-}, SO_4^{2-}, causes catalytic deactivation.	(Han and Yan, 2014)
Au–Ag	2/3/4–Nitrophenols	Au:Ag 1:5	4–Nitrophenol 95% (6 min); 3–Nitrophenol 64% (12 min); 2–Nitrophenol 75% (10 min)	–	High NO^* and OH^* scavenging activity promotes catalytic performance and enables rapid degradation of nitro phenols	(Kumari et al., 2015)
Ni–Fe	DDT	Ni:Fe 1:3.5 of 0.05 g//L for initial DDT conc. 1.09 μg/mL	90% of degradation within 4 h at pH 7	$4 \leq pH < 7$; $7 < pH \leq 10$	Higher pH >10 and lower pH<4 lowers the dehydrochlorination efficacy due to formation of precipitate and enhancement of corrosiveness at higher or lower pH respectively. pH<10 favours catalytic activity of Ni for electron transfer from ferric hydroxide to iron.	(Tian et al., 2009)
Fe–Mn oxide	Phosphate	Fe–Mn molar ratio of 5:1 of 2.5 g/L for initial PO_4^{3-} conc. 10–100 mg/L	Maximum adsorption capacity of 18.4 mg/g at 308 K and pH 7.0	5.0	pH plays important role in PO_4^{3-}sorption. Presence of coexisting anions do not impose any negative effect on removal suggesting the role of inner-surface sphere complexes in the adsorption process.	(Du et al., 2017)
Pt–Cu	Rhodamine B	Pt–Cu molar ratio 1:1.3; of 6 mg/mL for initial dye conc. 1×10^{-5} M.	Degraded to colorless form within 1 min high rate constant value of 4.5 × 10–2/*sec* obtained	7.0	Dye (RhB) serve as an electrophilic specie while BH_4^- act as a nucleophile which transfer electron to the bimetal and this electron accepted by RhB and thus leads to catalytic reduction degradation.	(Singh et al., 2013)
Ni–Al	Fluoride	Ni–Al molar ratio 2:1; of 2 g/L; for initial F^-conc. 2–20 mg/L	99.55% within 20 min at 30 °C	6.0	Presence of abundant hydroxyl ions on adsorbent surface participated in ion exchange with F^-	(Raghav et al., 2019)

(*continued on next page*)

Table 1 (*continued*)

Bimetal/ Bimetal oxides	Pollutant	Dosage of catalyst & initial conc. of pollutants	Removal Efficiency	Optimum pH	Research Highlights	Reference
Mg–Zn	Chromium(VI)	Mg–Zn 25:75% (W_{Mg}/W_{Zn}), of 10 g/L for initial Cr(VI) conc. 50 mg/L	97.10% (for batch) & 94.5% (for flow) within 10 min at 40 °C	3.0	The redox reaction initiated by Mg & Zn ions responsible for toxic Cr(VI) reduction into non toxic Cr(III)	(Rahimi et al., 2021)
ZrO_2 –LaO_x	As(III) & As(V)	ZrO_2 –LaO_x ZrO_2@50%$La(OH)_3$; of 1.0 g/L for initial arsenic conc.0.5–3.0 mM	Maximum arsenate/arsenite adsorption capacity 80.99 mg/g & 45.55 mg/g, respectively at 25 °C & 24 h of reaction time	7.0 (arsenate); 9.2 (arsenite)	The stability of LaO_X enhanced by addition of ZrO_2 which therefore preserved the adsorption sites at all pH values and thus retained removal efficiency	(Prabhu et al., 2020)
Al–ZnO	Pb(II)	Al (15 mol%) doped ZnO; of 1.0 g/L; for initial Pb conc. 50 mg/L	Maximum adsorption capacity 56 mg/g and 94% of removal observed at 25 °C within 5 h of reaction time	4.0	Doping of Al ions enhanced the surface charge density which thus modified its stability. Chemisorption mechanism govern the removal of Pb(II).	(Jawed and Pandey, 2019)
Cu–Ni supported on functionalized graphene oxide(GO)	p-nitrophenol	Cu:Ni (1:1); of 3.0 mg/30 mL; for 5 mM *p*NP conc.	100% conversion and selectivity within 16 min	Without pH adjustments	Due to good dispersion of 1:1 Cu-Ni bimetals over the functionalized support enhanced the interaction of pNP with GO through π-π bonding & facilitates reduction from the abstracted H^+ of BH_4^- & its subsequent transfer to the nitrophenolate ions.	(Rana and Jonnala-gadda, 2017)
Calcium alginate encapsulated Ni–Fe	Monochlorobenzene (MCB)	1.0 g/L in 50 mg/L of MCB	98.6% in 120 min at 308 K high rate constant value of 0.4178 min^{-1}	3.0–5.0	The Fe^0 initiate redox process by reacting with water to produce H_2 gas and results in dechlorination of MCB into benzene while Ni supported corrosion reaction	(Kuang et al., 2015)
Ca–Ti oxide	U(VI)	0.1 g/L for 30 mg/L of initial U(VI) conc.	90% removal efficiency at 298.15 K within 60 min.	4.0	The presence of coexisting ions not affects the U(VI) removal suggesting the formation of inner sphere complexes during removal process	(Hu et al., 2017)
$CuCo_2O_4$	Atrazine	$CuCo_2O_4$ (2:1) of 150 mg/L for initial atrazine conc. 5 mg/L	> 99% removal within 30 min of contact time at 30 °C	6.8	$SO_4^{\cdot-}$, OH^- radical play important role in the degradation process. The use of bimetal oxide activates peroxymonosulphate to release $SO_4^{\cdot-}$ which attacked the side chain of atrazine.	(Yin et al., 2021)
Magnetic chitosan support Co–Ni	2,4–dichlorophenoxyacetic acid (2,4–D)	Co–Ni (1:1) of 10 mg for 100 mg/L of 2,4–D	95.50% within 60 min of reaction time and rate constant value of 0.07517 min^{-1}	7.0	The degradation process initiated by H_2O_2 which oxidizes Co(0) into Co(II) and thus the later got oxidized further by H_2O_2 and produces ·OH radical and similarly Ni also get oxidized to produce ·OH. These ·OH radical finally break down 2,4–D	(Sharma et al., 2020)
Kaolin supported $CuCo_2O_4$	Phenacetin (PNT)	Cu–Co (1:1.18) of 0.1 g/L for 10 mg/L of PNT	100% degradation within 10 min and 58% removal of total organic carbon & degradation rate constant value 0.4 min^{-1} at 25 °C	7.0	·OH and $SO_4^{\cdot-}$ radicals activated by the bimetal drive the breakdown of PNT.	(Liu et al., 2020)

(*continued on next page*)

Table 1 (*continued*)

Bimetal/ Bimetal oxides	Pollutant	Dosage of catalyst & initial conc. of pollutants	Removal Efficiency	Optimum pH	Research Highlights	Reference
Fe–Ni	Tetracycline (TC)	Fe–Ni (20:1) of 0.1 g/L for initial TC conc. 50–500 mg/L	97.4% removal and 80% reduction of total organic removal within 2 h of contact time at 25°C	5.0	Presence of coexisting ions particularly NO_3^- decrease the catalytic activity by fouling the specific active sites of the catalyst.	(Dong et al., 2018)
Graphene wrapped nZVI–doped amorphous Al	Chloramphenicol (CAP)	nZVI–Al (16:1) of 0.5 g/L for initial CAP conc. 5–30 mg/L	93% of CAP removal (when activation occur via dissolve oxygen) 100% of CAP removal (Ar atmosphere) initial conc. 5 mg/L; reaction equilibrium time 120 min	3–10	The Al^{3+} component of the bimetallic system triggers the generation of reactive singlet oxygen species from dissolve oxygen and responsible for CAP degradation	(Yang et al., 2021)

Table 2
Bimetal/Bimetal oxide nanoparticles for the removal of HOC's and pathogenic microbes.

Material	Application	Reference
Nano Fe–Pd bimetal	Hydrodechlorination of chlorinated ethanes	(Lien and Zhang, 2005)
Nano Pd–Fe bimetal	Dechlorination of monochloroacetic acid in drinking water	(Chao et al., 2008)
Nano Fe–Pd bimetal	Reductive dechlorination of γ-hexachlorocyclohexane	(Nagpal et al., 2010)
Nano Pd–Fe bimetal	Catalytic dechlorination of 2,4-dichlorophenol	(Zhang et al., 2010)
Pd–Fe bimetal	Dechlorination of chlorinated methane	(Wang et al., 2009)
Nano Ni–Fe bimetal	Remediation of polybrominated diphenyl ethers in soil	(Xie et al., 2014)
Ni–Fe bimetal nanoparticles	Degradation of trichloroethylene from water	(Tee et al., 2005)
Ni–Fe bimetal nanoparticles	Removal of bromine from brominated phenyl ethers	(Fang et al., 2011)
Cu–Fe bimetal nanoparticles	Effective removal of chlorine from Hexachlorobenzene	(Zhu et al., 2010)
Cu–Fe bimetal nanoparticles	Reductive dechlorination of hexachlorobenzene	(Zheng et al., 2009)
$Zn_{0.05}$–Ag–Y bimetal	Microbial growth inhibition Escherichia coli and Saccharomyces cerevisiae	(Ferreira et al., 2015)
Ag–Zn@A–type zeolite	Inhibitory effects against Aspergillus niger	(Pereyra et al., 2014)
Cu–Ni@NaP zeolite	Antibacterial agents (E. coli/B. subtilis)	(Behin et al., 2016)
TiO_2–Ag@Zeolite-A based coating	Antimicrobial agent	(Nosrati et al., 2015)
Zn–Ag@Y zeolite	Growth inhibition of C. albicans, E. coli, and S. aureus	(Ferreira et al., 2016)
ZnO–CuO@Zeolite	Antibacterial agent for E. coli/B. subtilis	(Alswat et al., 2017)
Acrylic resins with incorporated Ag–Zn@zeolite	Antimicrobial agent (C. albicans/S. mutans)	(Casemiro et al., 2008)
AgBr–TiO_2@zeolite	Antibacterial agent for E. coli	(Padervand et al., 2012)
Ag/TiO_2@Montmorillonite	Photocatalytic degradation of E. coli	(Wu et al., 2010)
Ag–ZnO@Halloysite Nanotubes	Enhanced antibacterial activity for E. coli	(Shu et al., 2017)
Cu–Zn@montmorillonite	Antimicrobial and cytotoxicity	(Jiao et al., 2017)
Ag–Cu bimetal nanoparticles	Antimicrobial for E. coli/S. aureus	(Singh et al., 2014)
CNFs–Sn–ZrO_2 nanofibers	Improved supercapacitor and antibacterial activity (E. coli)	(Jang et al., 2014)
Cu/Zn@CNFs	Potential antibiotic material	(Ashfaq et al., 2016)
Cu/Zn-carbon micro/nanofiber-polymer nanocomposite	Wound dressing biomaterial	(Ashfaq et al., 2017)
Co/Ag@Chitosan/Carbon black fibre	Bactericidal (E. coli)	(Ali et al., 2017)

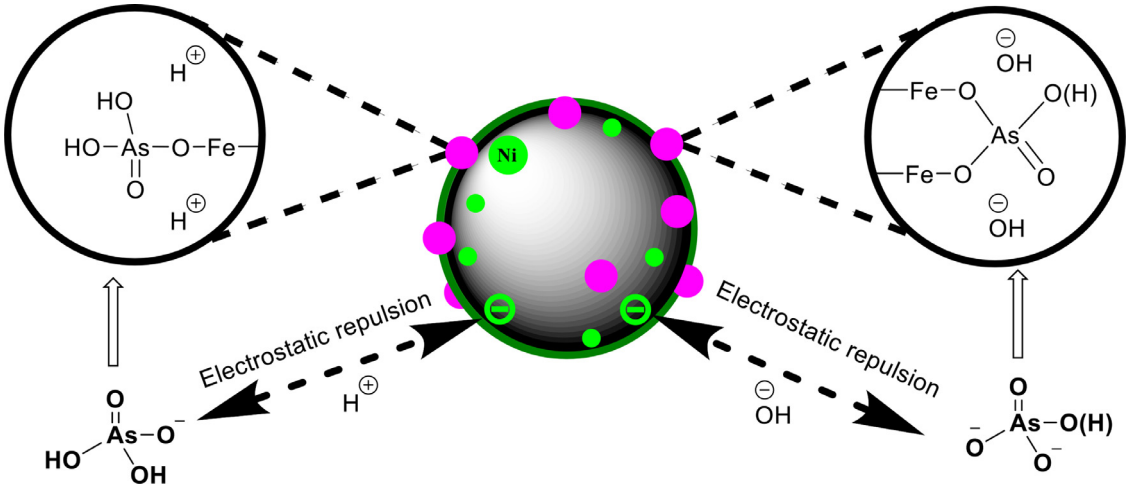

Fig. 4. Arsenic (V) removal mechanism.

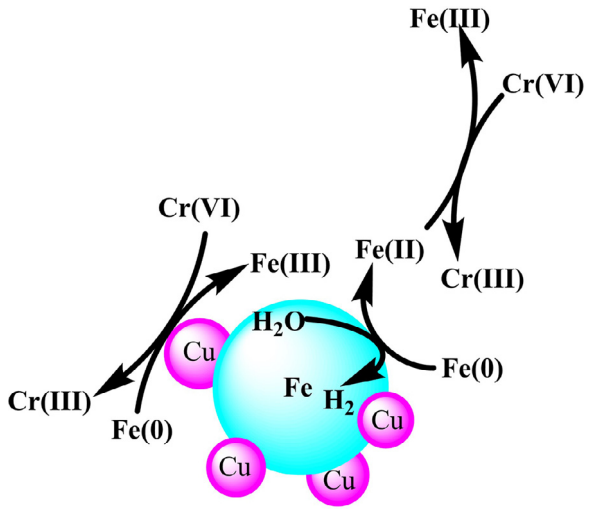

Fig. 5. Chromium (VI) removal using Cu–Fe bimetallic nanoparticles.

The chromium (VI) can be removed from wastewater using Cu–Fe bimetallic nanoparticles. The Cu–Fe bimetallic nanoparticles were prepared by liquid-phase chemical reduction, and the optimal Cu loading rate was 3% (wt%). The mechanistic interpretation of the removal process by XPS analysis revealed the reduction of Cr(VI) to Cr(III) and accumulated on the particle surface as $Cr(OH)_3$ (Fig. 5). The kinetics of the reaction followed a pseudo-second-order model and the removal efficiency decreased with increasing pH (Ye et al., 2021). In another report, the Fe–Sn nanoparticles deposited on talc were used as a potential adsorbent for the fast mitigation of Cr(VI). The Fe–Sn nanocomposite maintained a constant removal activity for 60 days (Bayat et al., 2021).

(b) Removal of heavy metals using bimetallic oxides

The bimetal oxides exhibit a superior adsorbent capacity in scavenging the heavy metal ions such as Co(II), Hg(II), and Cr(VI) from wastewater. The remediation mechanism of metal ions from wastewater by bimetals differs from bimetallic oxides because bimetallic oxides are usually employed as adsorbents in the process. The Cu–Mn oxide was prepared via the incipient wetness impregnation method and tested for the Hg removal capacity from natural gas and N_2. The bimetallic oxide can reduce Hg from 11,600 ppb to 0.1 ppb in a single pass. The developed method also tested to remove Hg from real natural gas and observed that H_2S present in the real natural gas improved the performance of the sorbent (Zhao et al., 2017). A Zn–Sn based mixed metal oxide was successfully applied to remove Cu^{2+}, Pb^{2+} and Sn^{2+} from contaminated water. Langmuir model best fit the adsorption kinetics, and the adsorbent dosage of 0.05 g and initial concentration of ions of 200 mg/L in 30 min was the best conditions to achieve maximum adsorption capacity of Cu^{2+} (38.92 mg/g), Pb^{2+} (117.16 mg/g) and Zn^{2+} (29.12 mg/g) (Honarmand et al., 2021). A Fe–Mn oxide supported clinoptilolite was applied for the enhanced Pb(II) removal. The adsorption of Pb(II) ions onto the Fe–Mn oxide surface fits better with the polymolecular adsorption model. The adsorption mechanism of Pb(II) onto hydrated Fe(III) and Mn(IV) oxides was explained through the Coulomb, hydrolysis, ion exchange, or coordination sorption models, as well as by a combination of all (Chmielewská et al., 2021).

(c) Removal of metalloids

Arsenic, selenium, and antimony are toxic, carcinogenic metalloids and their contamination in water are caused by anthropogenic activities and natural calamities. Bimetal oxides are frequently used as adsorbents for the removal of metalloids because of their large pore size, large specific surface area and mesoporous structure.

Arsenic contamination results in adverse health effects and carcinogenicity in human beings. Through the geochemical cycles, the As(V) and As(III) are easily enriched in water. The As(III) form is more toxic, soluble and mobile (Dutta et al., 2021). Adsorption reactions that occur on the surface of the minerals play a critical role in arsenic immobilization. Xie et al. developed a method for arsenic sequestration using a Fe–Mn composite oxide. A template-free route and high-temperature calcination synthesized the mesopore composite. Different Fe/Mn molar ratios and calcination temperatures were screened to synthesize a Fe–Mn composite with the largest specific surface area. The Fe1Mn1–300 showed the adsorption capacity of 59.44 mg/g for As(III) and 31.68 mg/g for As(V), and the mechanism of the removal was included adsorption co-precipitation and oxidative chelation (Xie et al., 2022). In a similar method, a series of ordered mesoporous Fe–Mn bimetal oxides (OMFMs) were synthesized using the inverse micelle method and evaluated for arsenic sequestration. The maximum adsorption capacity of 174.59 mg/g for As(III) and 134.58 mg/g for As(V) was achieved using a variant of OMFMS (OMFM–3). The mechanistic investigations revealed that the manganese oxides in OMFM–3 act as a potential As (III) oxidant and iron oxides serve as an adsorbent (Lu et al., 2021). The Fe–La oxide magnetic microspheres were successfully applied for the As(V) removal. The adsorption kinetics followed an intraparticle diffusion model, and the Langmuir model was well fitted for the adsorption isotherm. At pH 4, the maximum adsorption capacity of 62.32 mg/g for As(V) was achieved. The adsorption mechanism was probed using FT-IR and XPS, the As(V) adsorption ascribed to the ligand exchange and surface complex formation (Yan et al., 2020).

Antimony (Sb) is a priority control pollutant and potentially toxic to humans (Liu et al., 2021d) . The antimony compounds interfere with the enzymatic activity and induce hypoxia and metabolic disorders in natural aquatic environments. Antimony exists in Sb(III) and Sb(V). Although the mobility and solubility of Sb(V) are greater than Sb(III), the Sb(III) is ten folds toxic than Sb(V) (Li et al., 2018). The Fe–Zr bimetallic oxide was utilized to remove antimonate (Sb(V)). The Sb(V) adsorption kinetics operated via a pseudo-second-order rate and through an endothermic reaction. At high concentrations CO_3^{2-} and SiO_4^{4-} significantly inhibited the adsorption process (Li et al., 2012). The Fe–Mn bimetallic oxide nanoparticles supported on Al_2O_3 were applied for the oxidation and sorption of Sb(III). The nature bonding between Fe–Mn bimetallic oxide and Al_2O_3 is intermolecular hydrogen bonding and resulted in exceptional oxidation and sorption performance. The lattice Mn(IV) within the nanocomposite drives the oxidation of the Sb(III) to Sb(V), whereas FeOOH and Al_2O_3 act as sorption sites. The Fe–Mn@Al_2O_3 is reusable and exhibited excellent Sb(III) removal efficiency for five cycles (Bai et al., 2020). An interesting method for the co-removal of As(V) and Sb(V) was reported using Fe–Cu oxide. The Fe–Cu (2:1) oxide was an optimal proportion and exhibited a higher co-adsorption capacity of 70.9 mg/g for As(V) and 94.3 mg/g for Sb(V). The mechanism of the co-removal revealed that Cu provided an external force field mutual attraction for As(V) and Sb(V) over electrostatic repulsion (Wang et al., 2022).

In nature, selenium (Se) mainly exists as elemental selenium (Se^0), selenide (Se^{2-}). selenate (SeO_3^{2-}), and selenite (SeO_4^{2-}). Selenium oxyanions (Se(IV) and Se(VI)) are non-odoriferous and exhibit high mobility, ready bioaccumulation, and can induce teratogenic and mutagenic defects. The speciation of selenium is highly dependent on the pH and the redox potential. Under strong oxidizing conditions, SeO_4^{2-} is the dominant species, while under mild oxidizing conditions, $HSeO_3^-$ and SeO_3^{2-} are the main species. Under reducing conditions, volatile (H_2Se) and Se(0) would be prevalent. The remediation of selenium from wastewater is highly challenging (Sharma et al., 2019b) . A reusable Mg–Al bimetallic oxide ($MgAl_2O_4$) was utilized for selenite removal from the contaminated ground water. The spinal structure $MgAl_2O_4$ was synthesized by calcinating Mg/Al layered double hydroxides at 500 °C for 5 h. The $MgAl_2O_4$ showed a higher selenite adsorption capacity of 179.59 mg/g at 298 K and followed pseudo-second-order kinetics

(Possibility of chemisorption). Homogeneous adsorption is illustrated based on the predicted adsorption equilibrium by the Langmuir model (Tian et al., 2017). A method (best used at pH < 8) for the removal and in-situ immobilization of Se(IV) in ground water/soil was described using starch or carboxymethyl cellulose stabilized Fe–Mn bimetallic oxide. The starch stabilized Fe–Mn bimetallic oxide nanoparticles displayed the Langmuir adsorption capacity of 109 mg/g (Xie et al., 2015).

(d) Radionuclide removal

Uranium, Cobalt, Neodymium Gadolinium are the common radionuclides present in nuclear waste. Because of the high cytotoxicity, these radionuclides can cause a considerable threat to living organisms and environmental safety.

A method for the removal of UO_2^{2+} was reported using $MnFe_2O_4$@TpPa-1 (MFTP). The TpPa-1 is comprised of β–ketoenamine linked covalent organic frameworks and serves as supporting material and alleviate the aggregation of $MnFe_2O_4$. The adsorption of the U on MFTP was confirmed from the peaks at 393.08 (4f7/2) and 382.32 (4f5/2) eV in the XPS spectra. The MFTP exhibited a maximum adsorption capacity of 1235.01 mg/g. The adsorption mechanism involves the surface complexation and redox reaction (Zhong et al., 2021). The $CaTiO_x$ and $CaAlO_x$ were synthesized via a facial calcination method and successfully used to remove U(VI). At lower pH, the sorption mechanism was led by inner-sphere surface complexation, and at high pH, the mechanism switched to surface complexation. The chemisorption is the rate-controlling mechanism, and the Langmuir model well simulated the sorption isotherms (Hu et al., 2017).

The Fe–Mn bimetal oxide adsorbent was successfully applied for the removal of Co(II). The Fe–Mn adsorbent was amorphous with a surface area of 316.762 m^2/g. The Fe(III) centre drives the principle adsorption ability, and the Mn(IV) leads the oxidation of Co(II). The oxidation of Co(II) to Co(III) was confirmed using XPS measurements (Jiang et al., 2015).

The Fe(III)–Ti(IV) oxide was employed for the removal of Ce(III), Nd(III) and Gd(III) ions. The adsorption kinetics followed the pseudo-second-order model and isotherms were well simulated with the Freundlich model (Metwally and Rizk, 2014).

5. Removal of organic pollutants

5.1. Halogenated organic compounds (HOC's)

Natural and Synthetic Halogenated Organic Compounds (HOC's) are the largest group of environmental pollutants. The properties of the HOC's can be easily modified by varying the degree of halogenation and molecular structure (Xu et al., 2021a) .

(a) Use of bimetals in the removal of halogenated organic compounds (HOC's)

The magnetic Cu–Ni bimetallic particles embedded carbon sheets (C@Cu–Ni) utilized as a catalyst for the degradation of 2,4,6–trichlorophenol by peroxymonosulfate (PMS). The C@Cu–Ni promotes the PMS activation and facilitates the generation of the reactive oxygen species (ROS). The ROS was responsible for the rapid degradation of 2,4,6–trichlorophenol (Fig. 6). The C@Cu–Ni exhibited excellent reusability and degradation efficiency up to five catalytic cycles (Zhang et al., 2021a) .

In a similar report, Fe–Ni bimetallic particles supported by polystyrene resin (Fe/Ni-D072) were used for the degradation of 2,4–dichlorophenol (2,4-DCP). The presence of humic acid and CO_3^{2-} inhibit the degradation efficiency of Fe/Ni-D072. The degradation mechanism included the Ni catalyzed hydrogenolysis, and Fe@resin promoted adsorption of the final product (Zhang et al., 2021c) . The Fe–Zn bimetal was used in the high energy planetary ball mill process to mechanochemically destruct 1,1,1-trichloro-2,2-bis(p-chlorophenyl)-ethane (DDT). The rotation speed influenced the mechanochemical

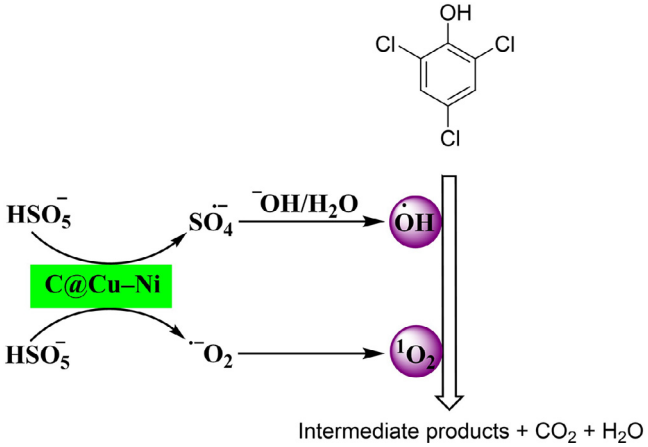

Fig. 6. C@Cu–Ni assisted PMS activation and degradation of 2,4,6–trichlorophenol.

(MC) destruction, and the charge ratio (mass of mill balls to materials), the rotation speed of 350 rpm and charge ratio of 35:1 was optimal to achieve 94% MC destruction of DDT within 1 h (Sui et al., 2018).

The Cu–Fe bimetal was successfully applied for the reductive dechlorination of haloacetamides (HAcAms). In the pH range 6.0–8.0, the Cu–Fe bimetal (>5.0 g/L) would be able to completely degrade trichloroacetamide (TCAcAm), dichloroacetamide (DCAcAm), and monochloroacetamide (MCAcAm) in 24 h. The high catalytic efficiency of the Cu–Fe bimetallic system is attributed to the efficient electron transfer between Cu and Fe (Chen et al., 2018).

The debromination of 2,3,4-tribromodiphenyl ether (BDE–21) was studied using Fe–Ag and Fe–Pd bimetals. The debromination proceeds via the removal of meta–bromine and leads to the formation of 2,4-dibromodiphenyl ether (BDE-7). The degradation kinetics followed a pseudo-first-order rate. The mechanism of the debromination was established based on the solvent kinetic isotope effect; Fe–Pd promoted debromination proceeds via H–transfer; however, Fe–Ag assisted debromination underwent through an electron-transfer (Wang et al., 2018).

(b) Use of bimetal oxides removal of halogenated organic compounds (HOC's)

A Fe–Mn oxide ($Mn_{1.5}FeO_{6.35}$) activated oxone was used for in situ chemical oxidation of trichloroethylene (TCE) in ground water. The $Mn_{1.5}FeO_{6.35}$ was synthesized by the calcination of $Mn_3[Fe(CN)_6]_2$ at 400 °C. The TCE degradation was facilitated by the reactive oxygen species generated from the oxone activation. The superior activity of the Fe–Mn oxide is attributed to the uniformly arranged atoms of Fe (II and III) and Mn (III and IV), which could be reversibly oxidized and reduced in the same atomic sites. The interconnected porous structure of the $Mn_{1.5}FeO_{6.35}$ holds a larger surface area for the efficient adsorption of oxone and TCE and further facilitate electron communication across the surface (Yang et al., 2020b) .

The degradation of 1,2,3,4-tetrachloronaphthalene (CN-27) was studied using three rod-like Fe–Al composite oxides (FeAl-1, FeAl-5 and FeAl-10). The FeAl-5 and FeAl-10 exhibited almost similar degradation efficiency (DgE, 93.0 ± 1.2% vs 90.2 ± 1.4%) and much superior to the DgE of FeAl-1 (38.7 ± 1.4%). The superior reactivity of the FeAl-5 and FeAl-10 towards CN-27 is explained based on the higher ratios of electrophilic oxygen. The Fe–Al composite oxide materials were synthesized using an ethylene-glycol-mediated method combined with impregnation-burning (Liu et al., 2017). The mesoporous flower-like Co–Ce composite oxide was applied for the degradation of 1,2,4-trichlorobenzene (1,2,4-TrCB). The degradation rate of 1,2,4-TrCB followed a first-order reaction kinetics model. An ethylene glycol mediated process was used to synthesise Co–Ce composite oxide, TBAB, and urea

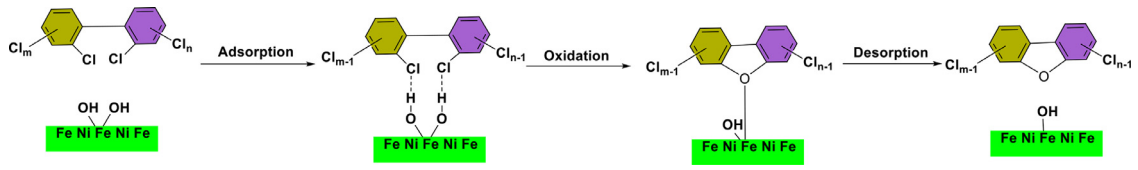

Fig. 7. $NiFe_2O_4$ assisted degradation of decachlorobiphenyl (CB–209) into PCDF.

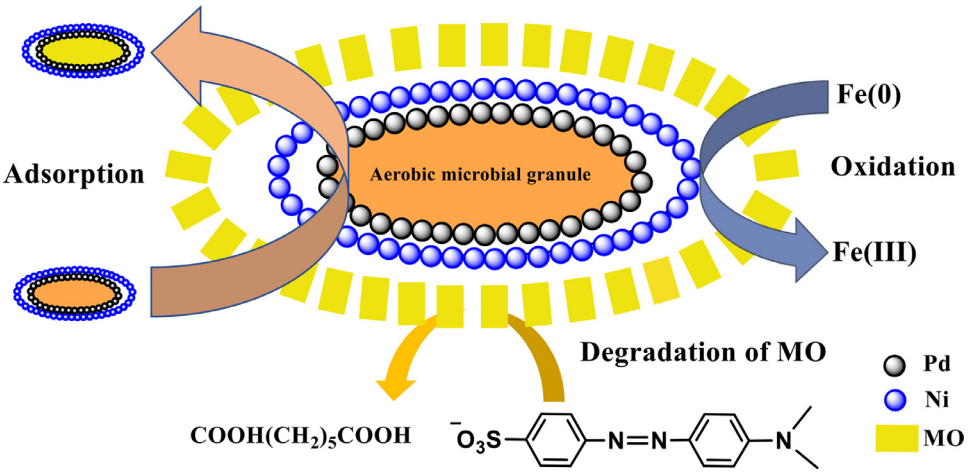

Fig. 8. Degradation pathway of MO using Bio-Pd–Fe.

was critical to achieve the flower-like structure and avoid the agglomeration (Lin et al., 2012). The spinel Ni–Fe bimetallic oxide ($NiFe_2O_4$) mediated decomposition of decachlorobiphenyl (CB–209) at 300 °C. The $NiFe_2O_4$ was prepared by coprecipitation and calcination at 400 °C for 3 h. The decomposition process of CB-209 by $NiFe_2O_4$ was eco-friendly due to the formation of significantly low levels of total polychlorinated-dibenzofurans (PCDF) (Fig. 7) (Huang et al., 2014).

5.2. Removal of dyes

Synthetic organic dye contamination is becoming an increasingly severe problem for the total environment and causing serious health risks. Synthetic organic dyes are the largest group of commercially available colouring substances. The textile, paper, printing, food, pharmaceutical, and cosmetic industries extensively depend on synthetic organic dyes to produce coloured products. The vast number of dyes made and their wide-ranging application areas generate a large volume of coloured wastewater and different types of post-production waste (Tkaczyk et al., 2020).

(a) Using bimetals

The bimetallic core-shell Pd–Fe nanoparticles on the surface of aerobic microbial granules (Bio-Pd–Fe) were successfully utilized for the 99.33 ± 0.2% removal of methyl orange from aqueous solutions. The impregnation of Pd–Fe onto the surfaces of microbial granules could provide more active sites for redox reactions as well as hydrogen generation and activation (Fig. 8) (Kubendiran et al., 2021).

A highly stable and heterogeneous Cu–Fe bimetallic catalyst supported on MCM–41 was applied for the photo–Fenton degradation of Orange II over a wide pH range. At pH 3, Cu–Fe@MCM-41 was succeeded to remove 93% of the total organic carbon (TOC) for the photo-Fenton degradation of Orange II and sustained its catalytic activity up to 10 consecutive runs (Lam and Hu, 2013).

(b) Using bimetal oxides

The photocatalytic performance of Ca–Fe bimetallic oxide ($Ca_4Fe_9O_{17}$) was utilized to degrade methylene blue (MB). The optical band gap of the $Ca_4Fe_9O_{17}$ was obtained as 1.9 eV from the Tauc plot using UV–vis absorption spectroscopy. The MB dye degradation efficiency of the photocatalyst was 57% under lower UV–visible light in 150 min (Chatterjee and Chakraborty, 2021).

The spinel $MnCo_2O_4$ supported on ordered mesoporous silica (SBA–15) ($MnCo_2O_4$@SBA–15) was evaluated for the activation of peroxymonosulfate (PMS) to degrade Rhodamine B (RhB) (Fig. 9). The Co–Mn/SBA-15 catalyst achieved 99% RhB removal efficiency in 45 min due to the Co–Mn synergistic catalytic effect (Xu et al., 2021b) .

The NiFe–oxide nanocubes were applied as adsorbents for organic dyes (284.99 mg/g for xylenol orange (XO), 31.97 mg/g for congo red (CR), and 57.66 mg/g for methylene blue) at 298 K. The adsorption kinetics was closer to the Liu isotherm model (Xie et al., 2019).

5.3. Removal of pharmaceuticals

Pharmaceuticals are emerging pollutants and pose a high environmental risk because of their bioaccumulation and the potential to act as bioactive compounds. The general prescription drugs are antibiotics, lipid regulators, β–blockers, analgesics, hormones, anti-inflammatory drugs, cholesterol-lowering statin drugs, and anti-depressants. The efficient removal of diverse pharmaceuticals from the aquatic system has been a formidable challenge due to the discrete physicochemical properties and occurrence at trace levels (Huang et al., 2021; Taoufik et al., 2021).

(a) Using bimetals

A low cost and ultrathin bimetallic nanoalloy of Cu–Bi supported on carboxylated multiwalled carbon nanotubes (c-CNTs) was synthesized and applied to degrade pharmaceuticals in water. The band gap energy (Eg) obtained from the Tauc plot is 2.60 and 2.50 eV for c-CNTs and CuBi/c-CNTs, respectively. The CuBi@MWCNTs catalyst was successfully applied for the visible-light-driven oxidation of Ciprofloxacin (CIP) and Ofloxacin (OFL). The photodegradation follows pseudo-first-order rate kinetics and adsorption isotherm well fitted with the Langmuir-Hinshelwood model. The degradation efficiencies of 93% for CIP and 91% of OFL was achieved over the CuBi@MWCNTs in 90 min (Khazaee et al., 2021).

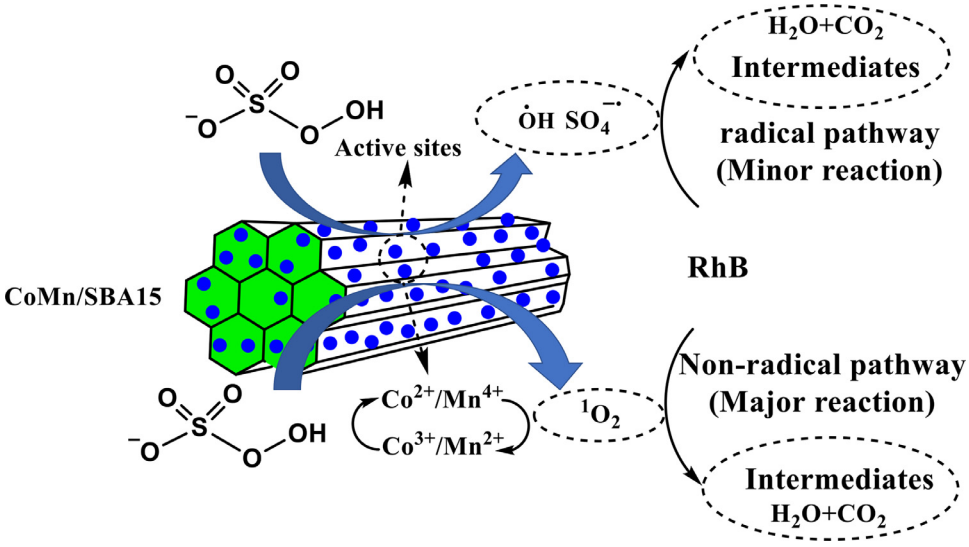

Fig. 9. $MnCo_2O_4$@SBA–15 mediated decomposition of RhB.

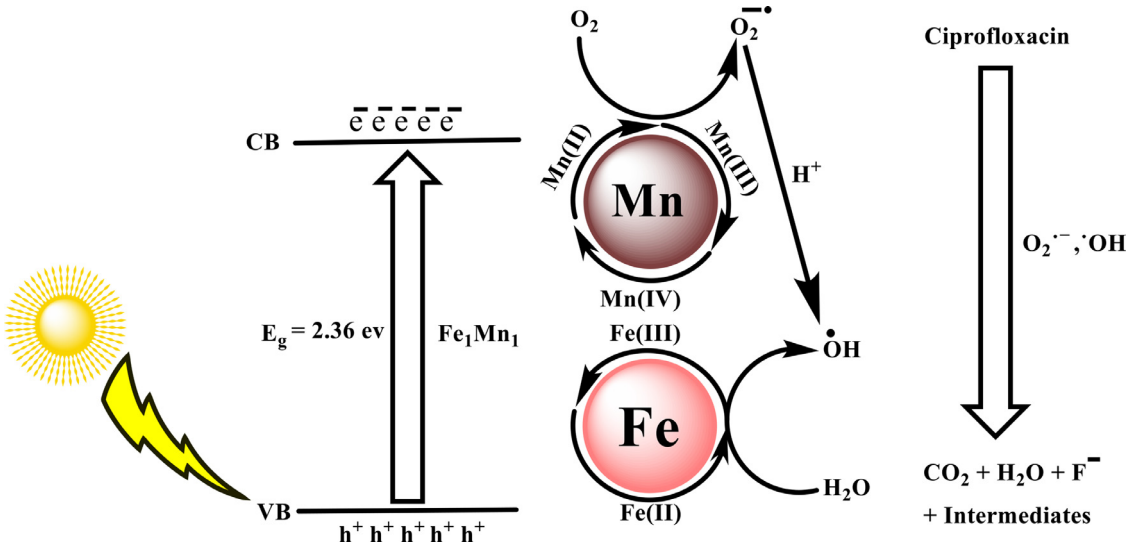

Fig. 10. Photocatalytic degradation of CIP.

The bimetallic semiconductor magnetic FexMny catalysts were synthesized via the impregnation method and utilized for the robust degradation of ciprofloxacin (98.3%), ofloxacin (96.0%), enrofloxacin (91.0%), levofloxacin (92.2%), and norfloxacin (93.5%). The Fe(III)–Mn(II) (1:1) catalyst displayed a highly porous structure and a large surface area of 122.5 m^2/g. The mechanistic investigation revealed that the $O_2^{\cdot-}$,$^{\cdot}OH$, h^+ is mainly responsible for removing the quinolones (Fig. 10) (Li et al., 2021b) .

The Fe–Ni bimetallic nanoparticles were synthesized and applied for the degradation of tetracycline (TC). The TC removal efficiency of 97.4% was achieved at pH 5. The presence of NO_3^- diminished the removal efficiency due to the possible redox reactions between NO_3^- and Fe/Ni BNPs (Dong et al., 2018).

The Zn and Fe nanoparticles supported on carbon nanotubes (Zn–Fe@NC) were fabricated via pyrolytic synthesis. The catalytic persulfate (PS) activation ability of Zn–Fe@NC was used to degrade sulfamethoxazole (SMX). The mechanistic investigations of the degradation revealed that the activation of the PS generated the reactive oxygen species ($^1O_2$), and $^1O_2$ was responsible for the SMX degradation (Yanan et al., 2020).

(b) Using bimetal oxides

The Cu and Fe bimetallic oxide impregnated on NaOH activated biochar (Fe–Cu/ABC) was synthesized and its catalytic activity was screened for ciprofloxacin (CIP) degradation via photo-electro-Fenton process at natural pH (92% removal of CIP in 8 h). The catalyst maintains its structural integrity up to 5 consecutive runs and exhibited excellent performance in 120 min to eliminate CIP from tap water (100%), river water (99.8%), and a real sample of pharmaceutical wastewater (91.74%) (Mansoori et al., 2021).

The Fe_3O_4–CuO_x hollow spheres (FCHS) was synthesized by depositing Fe_3O_4 on the shell of CuO_x hollow spheres prepared via a soft template method. The FCHS/persulfate (PS) exhibited excellent catalytic activity to degrade sulfadiazine (SDZ, 5 mg/L) (95%, $[catalyst]^0 = 0.2$ g/L, $[PS]^0 = 2$ mM, pH = 7.0) (Liu et al., 2021b).

The porous $CuCo_2O_4$ nanorods with dual enzyme activity were fabricated by annealing dual metallic MOFs. In the absence of H_2O_2, due to their oxidase-like property, $CuCo_2O_4$ nanorods can oxidize property2,2′-azino-di-(3-ethylbenzthiazoline sulfonic acid) (ABTS) and

3,3′,5,5′-tetramethylbenzidine (TMB), and develop green and blue products with maximum absorption at 419 nm and 652 nm respectively. The catalase like activity of $CuCo_2O_4$ nanorods was accessed from the decomposition of H_2O_2 (Song et al., 2020).

An electrochemical enhanced catalytic system was fabricated by placing $CoFe_2O_4$/ nickel foam (NF) in parallel between the anode and the cathode. The developed catalytic system was successfully utilized for the peroxymonosulfate (PMS) activation to remove levofloxacin (LVF). Under optimal conditions, more than 90% of LVF degradation was achieved within 40 min. The mechanistic investigation revealed that the excellent catalytic performances were due to the high generation ability of free radicals ($SO_4^{\bullet-}$, •OH and $O_2^{\bullet-}$) and non-radical ($^1O_2$) (Zhang et al., 2021b).

6. Removal of anions and oxyanions

Elevated levels of anions and oxyanions pose a serious threat to the environment, and they can cause detrimental effects to life on earth. The uncontrolled human and industrial activities within the environment provide access to these toxic anions and oxyanions to contaminate the water resources. Commonly encountered anions and oxyanion micropollutants in waste and surface water are fluoride (F^-), nitrate (NO_3^-), phosphate (PO_4^{3-}), perchlorate (ClO_4^-) and sulphate (SO_4^{2-}).

6.1. Bimetals in anions and oxyanions removal

The Mn(II)–La(III) bimetal was synthesized via coprecipitation method and applied for the highly pH-dependent decontamination of fluoride (F^-). The sorbent exhibited a maximum adsorption capacity of fluoride (292.9 mg/g) at pH. The presence of the coexisting anion phosphate strongly inhibited the adsorption process. The Langmuir model was the best fit for the adsorption isotherm and implied mono layer adsorption. The pseudo-second-order rate law best describes the experimental adsorption data with a correlation coefficient value of $r^2 = 0.98$ (Yu and Chen, 2014).

A Fe–Al bimetal chitosan bentonite (Fe–Al@bent) was fabricated and successfully applied to remove nitrate and its derivatives from wastewater at low temperatures (2–7 °C). The Fe–Al@bent removal efficiency of nitrate wastewater with a concentration of 50 mg/L was approximately 90% in 60 min (Cheng et al., 2020).

A rhenium–palladium bimetal catalysts on activated carbon support (Re–Pd@C) were synthesized and validated for an efficient reduction of ClO_4^- to chloride (Cl^-) under acidic conditions in waste ion-exchange (IX) regenerant brines. The excess NO_3^- deactivated the catalyst activity for the ClO_4^- reduction via the interaction with the *Re* component of the bimetal. The Re deactivation was avoided by pre-treating NO_3^- with In–Pd@Al_2O_3 (Liu et al., 2013).

The Cu–Pt foam electrodes were fabricated and applied to enhance the electrochemical reduction of nitrate. The Cu–Pt (180 s) electrode achieved 94% conversion of NO_3^- in 120 min yielding 194.4 mg NH_3–NL^{-1} $^gcat^{-1}$, with 84% selectivity for ammonia. The mechanistic investigations revealed that the Cu surface supports nitrate reduction to nitrite; platinum nanoparticles further enhance the conversion of nitrite to ammonia (Cerrón-Calle et al., 2021).

6.2. Bimetal oxides in anions and oxyanions removal

A method for the defluoridation of drinking water was reported using Al–Ce bimetal. The adsorbent was exhibited a high sorption capacity of 27.5 mg/g for fluoride at the equilibrium fluoride concentration of 1 mg/L. The adsorption isotherms were well aliened with the Langmuir model, and reaction kinetics followed a pseudo-second-order rate (Liu et al., 2010).

The needle-like Mg–La bimetal oxide nanocomposites were utilized for the cost-effective removal of phosphate and fluoride. The adsorption capacities for both phosphate (107.34 mg/g) and fluoride (63.11 mg/g) were achieved by Mg–La bimetal oxide at pH 4.0–6.0 (Kong et al., 2020).

A Fe–Ti bimetal oxide was synthesized with a Fe/Ti molar ratio of 20:1 using a coprecipitation method and applied as an optimal sorbent for phosphate removal. The reaction kinetics followed a pseudo-second-order rate law and implied chemisorption. The adsorption of phosphate was spontaneous and endothermic. The adsorption capacity calculated from the Langmuir equation was 35.4 mg/g at pH 6.8 (Lu et al., 2015).

7. Removal of pathogenic microbes and biotoxins

The contamination of water with pathogenic microorganisms (bacteria, viruses, fungi, and protozoa) and biotoxins can cause disease and death in human beings.

7.1. Using bimetallic nanoparticles

The removal of microcystins (MCY–LR, MCY–YR and MCY–RR) were studied using poly(propylene imine) dendrimers (G2 and G3) supported Fe/Ni bimetallic composites immobilized in polyethersulfone (PES) membrane (PES/G(x,y)FeNi). The membranes PES/G31FeNi and PES/G32FeNi were able to remove MCY–LR greater than 90% after 90 min of equilibrium time (Sivasankar et al., 2018).

The magnetic bimetallic Fe−Ag nanoparticles exhibit significant antibacterial and antifungal activities against disease-causing pathogens. The synthesis of Fe−Ag was carried out by direct reduction of silver ions zerovalent iron nanoparticles (nZVI). The antibacterial and antifungal activities of Fe−Ag nanoparticles were tested on ten different bacterial strains and four Candida species (Markova et al., 2013).

The Fe–Ni bimetal nanoparticles were synthesized and utilized to inactivate bacteriophage f2 in water under aerobic conditions. The synthesized Fe–Ni nanoparticles were spherical and existed as Fe(0) and Ni(0) and exhibited the highest removal efficiency with nanoparticles fabricated with a 5:1 Fe to Ni ratio (Cheng et al., 2019).

7.2. Using bimetallic oxide nanoparticles

Sivasankar et al. synthesized the spinel $ZnCr_2O_4$ (ZCO) nanoparticles and applied them to degrade cephalosporins. The optical band gap of 1.66 eV was calculated from the Tauc plot of UV–visible data. The ZCO photocatalytic degraded the cephalosporin family of compounds viz., Cefixime, Cefaclor and Cefuroxime up to 80.1%, 66.9% and 55.2%, respectively in 3 h (Benrighi et al., 2021).

8. Removal mechanisms of pollutants

Adsorption plays a crucial role in the removal of pollutants using modified/unmodified bimetal/bimetal oxides. The high surface area and enhanced porosity potentially increase the adsorption capacity of the bimetal/bimetal oxides. The tailoring of bimetal/bimetal oxides surface with various plant based or synthetic materials significantly tune up the adsorption capability of the sorbents and augment the interactions of the pollutants on the surface. The type of the interactions between the sorbent and pollutant decides the nature of the sorption. Physisorption result from the electrostatic interactions, hydrogen bonding, van der Waals interactions, and pore diffusion and chemisorption involve the ion exchange, microprecipitation, surface complexation, acid base interactions and chelation (Fig. 11). It has been observed that the general pollutant removal mechanism governed by pH based electrostatic interactions (Vilardi et al., 2019a). Electrostatic attractions/repulsions observed at various pH conditions and can be related with the pH_{ZPC} (zero point charge) of the bimetal/bimetal oxide. When $pH<pH_{ZPC}$, the protonation of the bimetallic surface facilitates anionic pollutant removal, where as removal of cationic pollutant favoured by the deprotonated condition observed at $pH>pH_{ZPC}$ (Fig. 12).

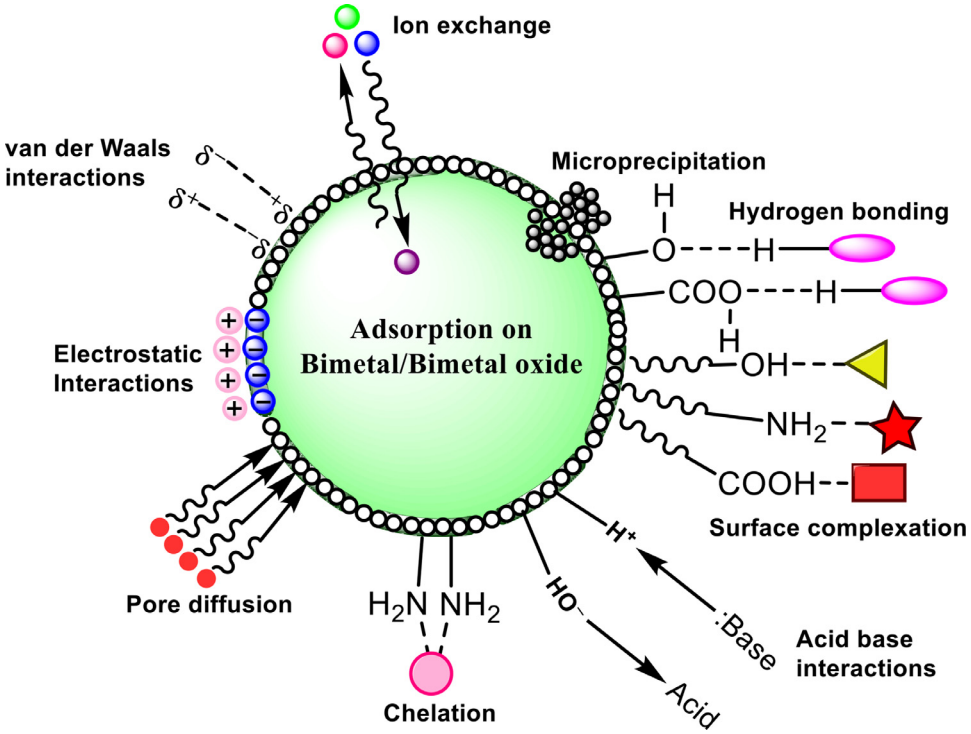

Fig. 11. Various mechanistic pathways for pollutants removal with bimetal/bimetal oxides.

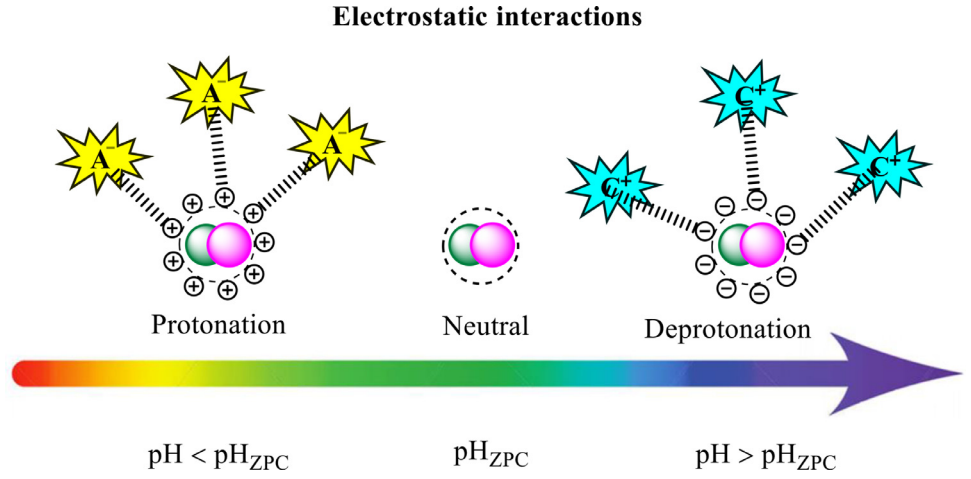

Fig. 12. Diagram representing electrostatic interactions based on zero-point charge (pH_{ZPC}) of bimetallics.

9. Economic and environmental considerations

The recycling and reusability scope of the bimetallic materials consider being an important aspect of the water treatment process. This regulates the total cost of the purification system and controls the potential environmental concerns that may arise from the direct discarding of the toxicants laden adsorbent into the environment. Numerous studies demonstrate that bimetallic materials can be efficaciously regenerated and can be used multiple times without significant loss in the adsorption capacity. However, a minor focus has been given to the recovery process using bimetallic materials. Limited studies are reported on the recovery aspect. The recovery of phosphate was successfully attempted using waste pine wood modified with Al-Ce nanocomposite. The recovery was made using 0.1 M NaOH solution followed by treatment with 0.1 M HCl solution. The phosphate recovery was observed more than 70% even after five successive regenerations (Nakarmi et al., 2020). Similarly, Liu research group demonstrated an enhanced phosphate recovery from the simulated urine samples using Mg/Fe bimetallic oxide modified biochar. The phosphate recovery efficiency was quantified as 70.4% even after five cycles of reuse, and the possible use of regenerated Mg/Fe biochar as a slow-release fertilizer was also reported (Liu et al., 2021a).

Several reagents of different concentrations were used for desorption and regeneration of the bimetallic materials such as NaOH, Na_2CO_3, NaCl, HCl, HNO_3, EDTA etc. For instance, the economic viability of chitosan-Cu-Fe complex for catalytic degradation of Reactive Black 5 in terms of its reusability prospect was examined by the research group of Rashid, in the presence of 0.4 mL H_2O_2 taking an initial concentration of 100 mg L^{-1} and adsorbent dose of 0.1 g at 6.5 pH. The reusability results demonstrated more than 80% removal efficiency even after 15 cycles (Rashid et al., 2015). A sugar-based carbon modified lanthanum and cobalt (La–Co@C) bimetal was used to degrade the methyl orange (MO). A regenerated La–Co@C exhibited more than 50% removal capacity for MO even after five recycling cycles. However, the removal performance decreases gradually with recycles due to the formation of irreversible active sites. The selection of appropriate solvents for desorption or regeneration reaction plays a vital role in this process (Liu et al., 2021c) . A report demonstrated that NaOH was used as an eluent for

Table 3
Reusability performance of different bimetal/bimetal oxides.

Bimetals/ Bimetallic oxides	Toxicants	Desorbing reagent	No of recycles	Reference
Fe–Ce bimetal oxide	Acid Orange 7	NaOH (0.1 M)	5	(Wen et al., 2019)
Fe–Mg bimetallic magnetic activated carbons	Malachite Green	Ethanol	4	(Guo et al., 2020)
Magnetic ZnO–Co_3O_4 bimetal oxide composite	Oxytetracycline	10% methanol, 20% acetonitrile, 70% 0.02 mol/L oxalic acid buffer	5	(Lian et al., 2017)
Bentonite-supported Fe–Ni bimetal	Mixed antibiotics amoxicillin, ampicillin and penicillin	Distilled water	5	(Weng et al., 2018)
Ginkgo biloba stabilized Fe–Co bimetal	Triclosan	Deionized water	8	(Gao et al., 2019)
Bimetallic Fe–Cu@ sepiolite composite	Ofloxacin	Water and ethanol	5	(Tian et al., 2020)
Indium tin oxide glass sheet supported Pt–Pd bimetal	Methyl parathion	Na	4	(Mahar et al., 2020)
Polymeric magnetic chitosan supported Co–Ni	2,4-dichlorophenoxy-acetic acid (2,4-D)	Ethanol	8	(Sharma et al., 2020)
$CuCo_2O_4$ activated Potassium peroxymonosulfate	Atrazine	Water	5	(Yin et al., 2021)
Hierarchical zinc–zirconium oxide	Fluoride	0.1 M NaOH	4	(Gao et al., 2020)
Ni–Al bimetallic	Fluoride	0.5 M NaOH	6	(Raghav et al., 2019)
Sn–Pd-red mud	Nitrate	Double deionized water	11	(Hamid et al., 2018)
TiO_2–nZVI	Nitrate	0.01 M NaOH	5	(Hejri et al., 2019)
Zero-valent Mg–Zn bimetal	Cr(VI)	0.1 M HNO_3	5	(Rahimi et al., 2021)
$MnFe_2O_4$	Cr(VI)	0.1 M NaOH	4	(Li et al., 2019)
Fe–Mn bimetal oxide	PO_4^{3-}	0.5 M NaOH	3	(Du et al., 2017)
Zn–Sn bimetal oxide	As(V)	0.1 M H_3PO_4	5	(Pazhoor et al., 2021)
Fe–Ce bimetal oxides	As(III)	0.5 M NaOH	6	(Wen et al., 2020)
Bimetallic Al-doped ZnO	Pb(II)	0.5 M NaOH	3	(Jawed and Pandey, 2019)
Cu–Ni bimetallic supported organo functionalized graphene oxide	p-nitrophenol	Distilled water	6	(Rana and Jonnalagadda, 2017)
Calcium alginate encapsulated Ni-Fe bimetal	Cu(II) and Monochlorobenzene	EDTA	3	(Kuang et al., 2015)
Fe/Ni Bimetallic Oxide Porous Graphene Composite	Sulfisoxazole	Acetonitrile	5	(Wang et al., 2021)
Kaolin-supported $CuCo_2O_4$	Phenacetin	Calcined at 500 °C	4	(Liu et al., 2020)
Zr–Ag nano organo-bimetallic	*Enterobacter hormaechei, Bacillus megaterium,* and *Bacillus bataviensis*	Sterilized normal saline water	5	(Gupta et al., 2021)
Humic acid incorporate Al–Zr bimetallic oxide	*E. coli* and *Staphylococcus aureus*	Dilute NaOH	5	(Nehra et al., 2020)

desorption of Sb(V) using Fe-Mn bimetal composite responsible for the phase transformation of the material from amorphous into a crystalline form which retarded adsorptive uptake of Sb(V). While with the use of 0.5 M NaOH and 0.5 M NaCl as an eluent, the chloride ions facilitate reprecipitation of iron oxides and result in higher adsorption-desorption efficacy. The regeneration possibilities of the bimetallic oxides loaded with radionuclide species were also explored by several researchers to understand the economic significance and to minimize the environmental impacts (Yang et al., 2020a) . The magnetic nano cubes of $MnFe_2O_4$ and hollow spheres of Fe_3O_4@MnO_x could be effectively used for the enrichment of U(VI) and Eu(III). The catalysts can be regenerated and operated for more than four consecutive cycles using 0.1 M NaOH and 0.5 M Na_2CO_3, respectively (Hu et al., 2018; Song et al., 2019). Desorption performance and regeneration competencies of the bimetallic species for different kinds of pollutants are represented explicitly in Table 3. Overall, it can be evident that almost all contaminants can be efficiently desorbed and regenerated in consecutive cycles. However, certain factors like the choice of desorbing reagents, the nature of interaction between the solute and the adsorbent, surface reactivity of the adsorbent, and chemical structure of the adsorbate found to be contributed significantly to regulating the efficacy of the regeneration process.

10. Essential concerns on the use of bimetallic based nanoparticles in water remediation

Although researchers have put little effort into dumping used bimetallic-based nano adsorbents after use, it is a paramount issue that competes with the increasing problems of recent technology. Generally, due to their novel and unique features, nanoparticles are frequently used to solve various environmental problems. The wide use of these bimetal nano adsorbents causes an inescapable crisis when they are emitted into the surroundings, especially into water bodies that further convey to the aquatic species. A well-organized assessment of the potential effects of these nano adsorbents while purifying water and ensuing sewage processing need urgent attention. Despite promising reports from available literature, the bimetallic based nano adsorbents face some deficiencies which may affect their usage in large scale treatment plants. Since they are needed in large amounts for industrial use, their availability is a significant concern. Furthermore, the cost of the treatment and catalyst is a major challenge (Din et al., 2019). Grave health risks arise because the commoner is ignorant of the improvement of modern technologies despite living in a developing world of nanotechnology; hence, they remain unaware of the toxicity caused by these nano adsorbents.

Therefore, the minimal cost in the synthesis route of bimetallic based nano adsorbents on a larger scale can improve their part in growing research concerns.

11. Limitations and future prospects of the bimetals and bimetal oxides

The recent synthesis techniques for both bimetals and bimetal oxides are frequently expensive as well as multifaceted.

The chemical methods of synthesis are commonly employed among all the techniques for the synthesis of bimetals. On the other hand, these methods are frequently carried out in the presence of toxic reductants and solvents. Even though the physical processes are green and

eco-friendly, they often entail the use of sophisticated equipment. The biological method utilizes environmentally friendly and non-toxic reducing agents. In the synthesis of bimetal oxides, the precipitation technique is generally employed. Although the precipitation technique is bedevilled by agglomeration, this challenge could be overcome by adding stabilizers and dispersants. Bimetallic based nanoparticles have specific morphology from metal precursors, and a porous structure can be efficiently prepared through the hydrothermal technique. The sol-gel is a facile and cheap technique used for the preparation of bimetal oxides. Yet, this technique requires calcination (Adeleye et al., 2016). Considering the spray pyrolysis method, the bimetal oxides can be efficiently prepared without much difficulty. However, an instrument for spraying of metal precursors and a high reaction temperature is required in this technique. Finally, the precipitation technique is favourable in the preparation of amorphous bimetal oxides; however, calcination temperature usually affects the specific area of the adsorbents.

Also, studies on multicomponent removal of pollutants under real-world settings are commonly overlooked in recent lab-scale research papers. Furthermore, the carbon dioxide generated by the oxidation of organic molecules is rarely evaluated. Advanced oxidation processes often create by-products that are much more hazardous than the original contaminants. Most of the researchers used batch systems to conduct wastewater treatment studies. Most practical systems, on the other hand, operate in a continuous mode. Hence, the need for more research using the fixed bed column (continuous mode) is required.

Future research may incline towards reducing cost by finding novel cheap materials, and developing facile feasible techniques. Furthermore, despite the fact that the utilization of these bimetallic based nano adsorbents in the remediation of pollutants from wastewater has achieved an apparent success nevertheless, the leaching of these metal ions from both bimetals and bimetal oxides calls for worries and concerns on factors such as the reduction of adsorbent longevity, high cost of the purification process (cradle to grave), and possible secondary metal pollution of the treated water. Hence, the need to explore and develop techniques for reducing metal leaching.

For the economic viability of a purification process via an accurate choice of bimetal and bimetal oxides for regeneration, extensive studies are necessary.

There is scarce literature on the practical/industrial application of bimetals/bimetal oxides. For this reason, mathematical modelling and simulation could be effective tools for predicting the behaviour and optimization of the whole process. This could involve the incorporation of different transport models, single-component models such as the Langmuir model, Sipp's model, and Freundlich model, or multi-component models such as the Dual Sorption Model (DSM), Ideal Adsorbed Solution Theory (IAST), and the Butler and Ockrent (BTM) Model in future adsorption studies.

Assessment of the function of the synthesized bimetal and bimetal oxide for continuous and large-scale application is a potential area of research.

Conclusion

The scarcity of adequate and drinking water has become an issue of great concern, especially in developing countries. This could be due to an increase in population, climate change, and prolonged drought. Bimetallic-based nanoparticles possess unique properties, such as large surface areas, shape, size, dimensions, and composition, which affect their catalytic properties, thereby making them more fascinating for water/wastewater treatment via the processes of adsorption disinfection and membrane separations. The review has explained the potential uses of bimetallic nanoparticles in removing pollutants from the wastewater as a promising candidate for present and future research. Escalation of the treatment efficiency can be achieved through tailoring of physical and chemical properties of the bimetallic materials. For the improvement of the physical property choice of a suitable synthesis technique is of paramount importance. Methods such as spray pyrolysis and radiolysis are highly effective, ecofriendly, and produce bimetallic with homogenous morphology in a well-segregated state. However, the cost of the synthesis process is the major limitation for its large scale application. The alleviation of chemical properties can be done through surface functionalization with suitable ligands or capping agents, which is also considered to be expensive and unsustainable for long term application. Hence, more research needs to be focused on designing cost-effective, environmentally compatible, and efficient bimetallic materials. The biological techniques recently used to synthesise bimetals are generally eco-friendly and economical, but upscaling the process is highly challenging. Even though the use of bimetallic based nanoparticles in wastewater remediation is characterized by the tremendous feat, it is still essential to enhance its efficacy by exploring more methods of reducing secondary metal contamination from leaching metal ions, high cost of synthesis and an increase in the reusability from these bimetals and bimetal oxides. Moreover, systematic life cycle assessment and associated risk assessment analysis is highly warranted to understand its ecotoxicological aspects.

Declaration of Competing Interest

The authors declared no conflicts of interest.

Acknowledgment

Dr. SB is thankful to Sharda University, Greater Noida, for financial support through Seed Fund Research Grant (1902–10). Dr. BKA is grateful to Rajiv Gandhi University, Arunachal Pradesh, for providing all essential facilities. The authors are also thankful to the anonymous reviewers for their insightful comments and suggestions.

References

Adekoya, J., Dare, E., Mesubi, M., Nejo, A.A., Swart, H., Revaprasadu, N., 2014. Synthesis of polyol based Ag/Pd nanocomposites for applications in catalysis. Result. Phys. 4, 12–19.

Adeleye, A.S., Conway, J.R., Garner, K., Huang, Y., Su, Y., Keller, A.A., 2016. Engineered nanomaterials for water treatment and remediation: costs, benefits, and applicability. Chem. Eng. J. 286, 640–662.

Ahuja, S., 2021. Water Quality worldwide, Handbook of Water Purity and Quality. Elsevier, pp. 19–33.

Alcântara, M.L., da Silva, J.S., Soares, R.O., Andrade, H.M., da Silva, L.A., Mascarenhas, A.J., 2018. Hydrothermal synthesis of bismuth niobates and their application in azo-dyes photo-discoloration. Mater. Res. Bull. 103, 166–172.

Alexander, K., Gajghate, S.S., Katarkar, A.S., Majumder, A., Bhaumik, S., 2020. Role of nanomaterials and surfactants for the preparation of graphene nanofluid: a review. In: Materials Today: Proceedings.

Ali, F., Khan, S.B., Kamal, T., Anwar, Y., Alamry, K.A., Asiri, A.M., 2017. Bactericidal and catalytic performance of green nanocomposite based-on chitosan/carbon black fiber supported monometallic and bimetallic nanoparticles. Chemosphere 188, 588–598.

Ali, S., Sharma, A.S., Ahmad, W., Zareef, M., Hassan, M.M., Viswadevarayalu, A., Jiao, T., Li, H., Chen, Q., 2021. Noble metals based bimetallic and trimetallic nanoparticles: controlled synthesis, antimicrobial and anticancer applications. Crit. Rev. Anal. Chem. 51 (5), 454–481.

Alswat, A.A., Ahmad, M.B., Saleh, T.A., 2017. Preparation and characterization of zeolite\zinc oxide-copper oxide nanocomposite: antibacterial activities. Colloid Interface Sci. Commun. 16, 19–24.

Anandan, S., Grieser, F., Ashokkumar, M., 2008. Sonochemical synthesis of Au– Ag core–shell bimetallic nanoparticles. J. Phys. Chem. C 112 (39), 15102–15105.

Ashfaq, M., Verma, N., Khan, S., 2016. Copper/zinc bimetal nanoparticles-dispersed carbon nanofibers: a novel potential antibiotic material. Mater. Sci. Eng. 59, 938–947.

Ashfaq, M., Verma, N., Khan, S., 2017. Highly effective Cu/Zn-carbon micro/nanofiber-polymer nanocomposite-based wound dressing biomaterial against the P. aeruginosa multi-and extensively drug-resistant strains. Mater. Sci. Eng. 77, 630–641.

Bai, Y., Wu, F., Gong, Y., 2020. Oxidation and adsorption of antimony (iii) from surface water using novel Al 2 O 3-supported Fe–Mn binary oxide nanoparticles: effectiveness, dynamic quantitative mechanisms, and life cycle analysis. Environ. Sci. 7 (10), 3047–3061.

Banerjee, S., Sharma, Y.C., 2019. Synthesis and application of Zn/Ce bimetallic oxides for the decontamination of arsenite (As-III) ions from aqueous solutions. J. Environ. Manage. 233, 151–164.

Bayat, M., Nasernejad, B., Falamaki, C., 2021. Preparation and characterization of nano–galvanic bimetallic Fe/Sn nanoparticles deposited on talc and its enhanced performance in Cr (VI) removal. Sci. Rep. 11 (1), 1–17.

Behin, J., Shahryarifar, A., Kazemian, H., 2016. Ultrasound-assisted synthesis of Cu and Cu/Ni nanoparticles on NaP zeolite support as antibacterial agents. Chem. Eng. Technol. 39 (12), 2389–2403.
Benrighi, Y., Nasrallah, N., Chaabane, T., Sivasankar, V., Darchen, A., Baaloudj, O., 2021. Photocatalytic performances of ZnCr2O4 nanoparticles for cephalosporins removal: structural, optical and electrochemical properties. Opt. Mater. (Amst) 115, 111035.
Cao, X., Wang, N., Jia, S., Guo, L., Li, K., 2013. Bimetallic AuPt nanochains: synthesis and their application in electrochemical immunosensor for the detection of carcinoembryonic antigen. Biosens. Bioelectron. 39 (1), 226–230.
Casemiro, L.A., Martins, C.H.G., Pires-de-Souza, F.d.C.P., Panzeri, H., 2008. Antimicrobial and mechanical properties of acrylic resins with incorporated silver–zinc zeolite–part I. Gerodontology 25 (3), 187–194.
Cerrón-Calle, G.A., Fajardo, A.S., Sánchez-Sánchez, C.M., Garcia-Segura, S., 2021. Highly reactive Cu-Pt bimetallic 3D-electrocatalyst for selective nitrate reduction to ammonia. Appl. Catal. B, 120844.
Chai, L., Wang, Y., Zhao, N., Yang, W., You, X., 2013. Sulfate-doped Fe3O4/Al2O3 nanoparticles as a novel adsorbent for fluoride removal from drinking water. Water Res. 47 (12), 4040–4049.
Chao, C., Xiangyu, W., Chang, Y., Huiling, L., 2008. Dechlorination of disinfection by-product monochloroacetic acid in drinking water by nanoscale palladized iron bimetallic particle. J. Environ. Sci. 20 (8), 945–951.
Chatterjee, P., Chakraborty, A.K., 2021. Metal organic framework derived Ca4Fe9O17 as photocatalyst for degradation of organic dyes. Mater. Lett. 284, 129034.
Chen, L., He, B.-Y., He, S., Wang, T.-J., Su, C.-L., Jin, Y., 2012. Fe—Ti oxide nano-adsorbent synthesized by co-precipitation for fluoride removal from drinking water and its adsorption mechanism. Powder Technol. 227, 3–8.
Chen, S., Chu, W., Wei, H., Zhao, H., Xu, B., Gao, N., Yin, D., 2018. Reductive dechlorination of haloacetamides in drinking water by Cu/Fe bimetal. Sep. Purif. Technol. 203, 226–232.
Cheng, H., Zhu, Q., Wang, A., Weng, M., Xing, Z., 2020. Composite of chitosan and bentonite cladding Fe–Al bimetal: effective removal of nitrate and by-products from wastewater. Environ. Res. 184, 109336.
Cheng, R., Kang, M., Zhuang, S., Wang, S., Zheng, X., Pan, X., Shi, L., Wang, J., 2019. Removal of bacteriophage f2 in water by Fe/Ni nanoparticles: optimization of Fe/Ni ratio and influencing factors. Sci. Total Environ. 649, 995–1003.
Chmielewská, E., Tylus, W., Bujdoš, M., 2021. Study of mono-and bimetallic Fe and Mn oxide-supported clinoptilolite for improved Pb (II) removal. Molecules 26 (14), 4143.
Dabala, M., Pollet, B., Zin, V., Campadello, E., Mason, T.J., 2008. Sonoelectrochemical (20 kHz) production of Co 65 Fe 35 alloy nanoparticles from Aotani solutions. J. Appl. Electrochem. 38 (3), 395–402.
Darmawan, A., Karlina, L., Astuti, Y., Wang, D., Motuzas, J., Da Costa, J., 2017. Interlayer free–nickel doped silica membranes for desalination. IOP Conference Series: Materials Science and Engineering. IOP Publishing.
De Souza, C.D., Nogueira, B.R., Rostelato, M.E.C., 2019. Review of the methodologies used in the synthesis gold nanoparticles by chemical reduction. J. Alloys Compd. 798, 714–740.
Dębski, A., Pęska, M., Dworecka-Wójcik, J., Terlicka, S., Gąsior, W., Gierlotka, W., Polański, M., 2021. Structural and calorimetric studies of magnesium-rich Mg-Pd alloys. J. Alloys Compd. 858, 158085.
Din, M.I., Nabi, A.G., Hussain, Z., Arshad, M., Intisar, A., Sharif, A., Ahmed, E., Mehmood, H.A., Mirza, M.L., 2019. Innovative seizure of metal/metal oxide nanoparticles in water purification: a critical review of potential risks. Crit. Rev. Anal. Chem. 49 (6), 534–541.
Dong, H., Jiang, Z., Zhang, C., Deng, J., Hou, K., Cheng, Y., Zhang, L., Zeng, G., 2018. Removal of tetracycline by Fe/Ni bimetallic nanoparticles in aqueous solution. J. Colloid Interface Sci. 513, 117–125.
Du, X., Han, Q., Li, J., Li, H., 2017. The behavior of phosphate adsorption and its reactions on the surfaces of Fe–Mn oxide adsorbent. J. Taiwan Inst. Chem. Eng. 76, 167–175.
Dutta, D., Borah, J., Puzari, A., 2021. Iron oxide coated hollow poly (methylmethacrylate) as an efficient adsorption media for removal of arsenic from water. RSC Adv. 11 (22), 13376–13385.
Eslami, H., Ehrampoush, M.H., Esmaeili, A., Ebrahimi, A.A., Ghaneian, M.T., Falahzadeh, H., Salmani, M.H., 2019. Synthesis of mesoporous Fe-Mn bimetal oxide nanocomposite by aeration co-precipitation method: physicochemical, structural, and optical properties. Mater. Chem. Phys. 224, 65–72.
Fang, Z., Qiu, X., Chen, J., Qiu, X., 2011. Debromination of polybrominated diphenyl ethers by Ni/Fe bimetallic nanoparticles: influencing factors, kinetics, and mechanism. J. Hazard. Mater. 185 (2–3), 958–969.
Feng, J., Liu, T., Xu, Y., Zhao, J., He, Y., 2011. Effects of PVA content on the synthesis of LaFeO3 via sol–gel route. Ceram. Int. 37 (4), 1203–1207.
Ferrando, R., Jellinek, J., 2009. Nano-particles as a catalysts incatalytic converters, RL Johnston. Chem. Rev 108, 845.
Ferreira, L., Almeida-Aguiar, C., Parpot, P., Fonseca, A.M., Neves, I.C., 2015. Preparation and assessment of antimicrobial properties of bimetallic materials based on NaY zeolite. RSC Adv. 5 (47), 37188–37195.
Ferreira, L., Guedes, J.F., Almeida-Aguiar, C., Fonseca, A.M., Neves, I.C., 2016. Microbial growth inhibition caused by Zn/Ag-Y zeolite materials with different amounts of silver. Colloids Surf. B 142, 141–147.
Fry, J.P., Love, D.C., MacDonald, G.K., West, P.C., Engstrom, P.M., Nachman, K.E., Lawrence, R.S., 2016. Environmental health impacts of feeding crops to farmed fish. Environ. Int. 91, 201–214.
Fu, F., Cheng, Z., Lu, J., 2015. Synthesis and use of bimetals and bimetal oxides in contaminants removal from water: a review. RSC Adv. 5 (104), 85395–85409.
Fu, F., Wang, Q., 2011. A review of removal of heavy metal ions from wastewaters. J. Environ. Manage. 92 (3), 407–418.
Gao, J.-F., Wu, Z.-L., Duan, W.-J., Zhang, .W..-Z., 2019. Simultaneous adsorption and degradation of triclosan by Ginkgo biloba L. stabilized Fe/Co bimetallic nanoparticles. Sci. Total Environ. 662, 978–989.
Gao, M., Wang, W., Cao, M., Yang, H., Li, Y., 2020. Constructing hydrangea-like hierarchical zinc-zirconium oxide microspheres for accelerating fluoride elimination. J. Mol. Liq. 317, 114133.
Gómez, E.I.L., Edalati, K., Antiqueira, F.J., Coimbrão, D.D., Zepon, G., Leiva, D.R., Ishikawa, T.T., Cubero-Sesin, J.M., Botta, W.J., 2020. Synthesis of nanostructured TiFe hydrogen storage material by mechanical alloying via high-pressure torsion. Adv. Eng. Mater. 22 (10), 2000011.
Gopal, K., Tripathy, S.S., Bersillon, J.L., Dubey, S.P., 2007. Chlorination byproducts, their toxicodynamics and removal from drinking water. J. Hazard. Mater. 140 (1–2), 1–6.
Guo, F., Jiang, X., Li, X., Jia, X., Liang, S., Qian, L., 2020. Synthesis of MgO/Fe3O4 nanoparticles embedded activated carbon from biomass for high-efficient adsorption of malachite green. Mater. Chem. Phys. 240, 122240.
Gupta, A.R., Ranawat, B., Singh, A., Yadav, A., Sharma, S., 2021. Zirconium-silver nano organo-bimetallic network for scavenging hazardous ions from water and its antibacterial potentiality: an environment-friendly approach. J. Environ. Chem. Eng. 9 (4), 105356.
Haller, L., Hutton, G., Bartram, J., 2007. Estimating the costs and health benefits of water and sanitation improvements at global level. J. Water Health 5 (4), 467–480.
Hamid, S., Bae, S., Lee, W., 2018. Novel bimetallic catalyst supported by red mud for enhanced nitrate reduction. Chem. Eng. J. 348, 877–887.
Han, T., Zhang, Y., Xu, J., Dong, J., Liu, C.-C., 2015. Monodisperse AuM (M= Pd, Rh, Pt) bimetallic nanocrystals for enhanced electrochemical detection of H2O2. Sens. Actuators B 207, 404–412.
Han, Y., Yan, W., 2014. Bimetallic nickel–iron nanoparticles for groundwater decontamination: effect of groundwater constituents on surface deactivation. Water Res. 66, 149–159.
Hao, S., Zhang, H., 2017. High catalytic performance of nitrate reduction by synergistic effect of zero-valent iron (Fe0) and bimetallic composite carrier catalyst. J Clean Prod 167, 192–200.
He, Z., Xiao, K., Durant, W., Hensley, D.K., Anthony, J.E., Hong, K., Kilbey, S.M., Chen, J., Li, D., 2011. Enhanced performance consistency in nanoparticle/TIPS pentacene-based organic thin film transistors. Adv. Funct. Mater. 21 (19), 3617–3623.
He, Z., Zhang, Z., Bi, S., 2020. Nanoparticles for organic electronics applications. Mater. Res. Express 7 (1), 012004.
Hejri, Z., Hejri, M., Omidvar, M., Morshedi, S., 2019. Synthesis of TiO 2/nZVI nanocomposite for nitrate removal from aqueous solution. Int. J. Ind. Chem. 10 (3), 225–236.
Honarmand, M., Amini, M., Iranfar, A., Naeimi, A., 2021. Green synthesis of ZnO/SnO 2 nanocomposites using pine leaves and their application for the removal of heavy metals from aqueous media. J. Cluster Sci. 1–10.
Hu, Y., Wang, X., Zou, Y., Wen, T., Wang, X., Alsaedi, A., Hayat, T., Wang, X., 2017. Superior sorption capacities of Ca-Ti and Ca-Al bimetallic oxides for U (VI) from aqueous solutions. Chem. Eng. J. 316, 419–428.
Hu, Y., Zhao, C., Yin, L., Wen, T., Yang, Y., Ai, Y., Wang, X., 2018. Combining batch technique with theoretical calculation studies to analyze the highly efficient enrichment of U (VI) and Eu (III) on magnetic MnFe2O4 nanocubes. Chem. Eng. J. 349, 347–357.
Huang, L., Shen, R., Shuai, Q., 2021. Adsorptive removal of pharmaceuticals from water using metal-organic frameworks: a review. J. Environ. Manage. 277, 111389.
Huang, L., Su, G., Liu, Y., Li, L., Liu, S., Lu, H., Zheng, M., 2014. Effect of NiFe 2 O 4 on PCDF byproducts formation during thermal degradation of decachlorobiphenyl. RSC Adv. 4 (48), 25453–25460.
Jang, Y.-S., Amna, T., Hassan, M.S., Gu, J.-L., Kim, I.-S., Kim, H.-C., Kim, J.-H., Baik, S.-H., Khil, .M..-S., 2014. Improved supercapacitor potential and antibacterial activity of bimetallic CNFs–Sn–ZrO 2 nanofibers: fabrication and characterization. RSC Adv. 4 (33), 17268–17273.
Jawed, A., Pandey, L.M., 2019. Application of bimetallic Al-doped ZnO nano-assembly for heavy metal removal and decontamination of wastewater. Water Sci. Technol. 80 (11), 2067–2078.
Jiang, L., Xiao, S., Chen, J., 2015. Removal behavior and mechanism of Co (II) on the surface of Fe–Mn binary oxide adsorbent. Colloids Surf. A 479, 1–10.
Jiang, X., Fan, X., Xu, W., Zhang, R., Wu, G., 2019. Biosynthesis of bimetallic Au–Ag nanoparticles using Escherichia coli and its biomedical applications. ACS Biomater Sci Eng 6 (1), 680–689.
Jiao, L., Lin, F., Cao, S., Wang, C., Wu, H., Shu, M., Hu, C., 2017. Preparation, characterization, antimicrobial and cytotoxicity studies of copper/zinc-loaded montmorillonite. J Anim Sci Biotechnol 8 (1), 1–7.
Jung, D.S., Park, S.B., Kang, Y.C., 2010. Design of particles by spray pyrolysis and recent progress in its application. Korean J. Chem. Eng. 27 (6), 1621–1645.
Kanan, S., Moyet, M.A., Arthur, R.B., Patterson, H.H., 2020. Recent advances on TiO2-based photocatalysts toward the degradation of pesticides and major organic pollutants from water bodies. Catal. Rev. 62 (1), 1–65.
Khazaee, Z., Mahjoub, A.R., Khavar, A.H.C., 2021. One-pot synthesis of CuBi bimetallic alloy nanosheets-supported functionalized multiwalled carbon nanotubes as efficient photocatalyst for oxidation of fluoroquinolones. Appl. Catal. B 297, 120480.
Kong, L., Tian, Y., Pang, Z., Huang, X., Li, M., Li, N., Zhang, J., Zuo, W., Li, J., 2020. Needle-like Mg-La bimetal oxide nanocomposites derived from periclase and lanthanum for cost-effective phosphate and fluoride removal: characterization, performance and mechanism. Chem. Eng. J. 382, 122963.
Kuang, Y., Du, J., Zhou, R., Chen, Z., Megharaj, M., Naidu, R., 2015. Calcium alginate encapsulated Ni/Fe nanoparticles beads for simultaneous removal of Cu (II) and monochlorobenzene. J. Colloid Interface Sci. 447, 85–91.
Kubendiran, H., Alex, S.A., Pulimi, M., Chandrasekaran, N., Nancharaiah, Y., Venugopalan, V., Mukherjee, A., 2021. Development of biogenic bimetallic Pd/Fe nanopar-

ticle–impregnated aerobic microbial granules with potential for dye removal. J. Environ. Manage. 293, 112789.
Kumari, M.M., Jacob, J., Philip, D., 2015. Green synthesis and applications of Au–Ag bimetallic nanoparticles. Spectrochim. Acta Part A 137, 185–192.
Lam, F.L., Hu, X., 2013. pH-insensitive bimetallic catalyst for the abatement of dye pollutants by photo-fenton oxidation. Ind. Eng. Chem. Res. 52 (20), 6639–6646.
Li, H., He, Z., Ouyang, Z., Palchoudhury, S., Ingram, C.W., Harruna, I.I., Li, D., 2020. Modifying electrical and magnetic properties of single-walled carbon nanotubes by decorating with iron oxide nanoparticles. J. Nanosci. Nanotechnol. 20 (4), 2611–2616.
Li, J., Xiao, G., Guo, Z., Lin, B., Hu, Y., Fu, M., Ye, D., 2021a. ZSM-5-supported V-Cu bimetallic oxide catalyst for remarkable catalytic oxidation of toluene in coal-fired flue gas. Chem. Eng. J. 419, 129675.
Li, J., Zheng, B., He, Y., Zhou, Y., Chen, X., Ruan, S., Yang, Y., Dai, C., Tang, L., 2018. Antimony contamination, consequences and removal techniques: a review. Ecotoxicol. Environ. Saf. 156, 125–134.
Li, N., Li, W., Fu, F., 2019. Removal of chromium (VI) by MnFe 2 O 4 and ferrous ion: synergetic effects and reaction mechanism. Environ. Sci. Pollut. Res. 26 (29), 30498–30507.
Li, X., Dou, X., Li, J., 2012. Antimony (V) removal from water by iron-zirconium bimetal oxide: performance and mechanism. J. Environ. Sci. 24 (7), 1197–1203.
Li, X., Yang, Z., Hu, D., Wang, A., Chen, Y., Huang, Y., Zhang, M., Yuan, H., Yan, K., 2021b. Bimetallic Fe x Mn y catalysts derived from metal organic frameworks for efficient photocatalytic removal of quinolones without oxidant. Environ. Sci. 8 (9), 2595–2606.
Li, Y., Li, X., Xiao, Y., Wei, C., Han, D., Huang, W., 2016. Catalytic debromination of tetrabromobisphenol A by Ni/nZVI bimetallic particles. Chem. Eng. J. 284, 1242–1250.
Lian, L., Lv, J., Lou, D., 2017. Synthesis of novel magnetic microspheres with bimetal oxide shell for excellent adsorption of oxytetracycline. ACS Sustain. Chem. Eng. 5 (11), 10298–10306.
Liang, G., Schulz, R., 2004. The reaction of hydrogen with Mg-Cd alloys prepared by mechanical alloying. J. Mater. Sci. 39 (5), 1557–1562.
Lien, H.-L., Zhang, W.-x., 2005. Hydrodechlorination of chlorinated ethanes by nanoscale Pd/Fe bimetallic particles. J. Environ. Eng. 131 (1), 4–10.
Lin, S., Su, G., Zheng, M., Ji, D., Jia, M., Liu, Y., 2012. Synthesis of flower-like Co3O4–CeO2 composite oxide and its application to catalytic degradation of 1, 2, 4-trichlorobenzene. Appl. Catal. B 123, 440–447.
Lin, Y., Jin, X., Khan, N.I., Owens, G., Chen, Z., 2022. Bimetallic Fe/Ni nanoparticles derived from green synthesis for the removal of arsenic (V) in mine wastewater. J. Environ. Manage. 301, 113838.
Liu, H., Deng, S., Li, Z., Yu, G., Huang, J., 2010. Preparation of Al–Ce hybrid adsorbent and its application for defluoridation of drinking water. J. Hazard. Mater. 179 (1–3), 424–430.
Liu, H., Shan, J., Chen, Z., Lichtfouse, E., 2021a. Efficient recovery of phosphate from simulated urine by Mg/Fe bimetallic oxide modified biochar as a potential resource. Sci. Total Environ. 784, 147546.
Liu, J., Choe, J.K., Sasnow, Z., Werth, C.J., Strathmann, T.J., 2013a. Application of a *Re*–Pd bimetallic catalyst for treatment of perchlorate in waste ion-exchange regenerant brine. Water Res. 47 (1), 91–101.
Liu, L., Li, Y., Pang, Y., Lan, Y., Zhou, L., 2020. Activation of peroxymonosulfate with CuCo2O4@ kaolin for the efficient degradation of phenacetin. Chem. Eng. J. 401, 126014.
Liu, S., Fan, M.-q., Wang, C., Huang, Y.-x., Chen, D., Bai, L.-q., Shu, K.-y., 2012. Hydrogen generation by hydrolysis of Al–Li–Bi–NaCl mixture with pure water. Int. J. Hydrogen Energy 37 (1), 1014–1020.
Liu, T., Wu, K., Wang, M., Jing, C., Chen, Y., Yang, S., Jin, P., 2021b. Performance and mechanisms of sulfadiazine removal using persulfate activated by Fe3O4@ CuOx hollow spheres. Chemosphere 262, 127845.
Liu, W.-J., Qian, T.-T., Jiang, H., 2014. Bimetallic Fe nanoparticles: recent advances in synthesis and application in catalytic elimination of environmental pollutants. Chem. Eng. J. 236, 448–463.
Liu, X., Chen, Z., Chen, Z., Megharaj, M., Naidu, R., 2013b. Remediation of Direct Black G in wastewater using kaolin-supported bimetallic Fe/Ni nanoparticles. Chem. Eng. J. 223, 764–771.
Liu, X., Wu, Y., Ye, H., Chen, J., Xiao, W., Zhou, W., Garba, Z.N., Lawan, I., Wang, L., Yuan, Z., 2021c. Modification of sugar-based carbon using lanthanum and cobalt bimetal species for effective adsorption of methyl orange. Environ. Technol. Innov. 23, 101769.
Liu, Y., Lu, H., Pan, W., Li, Q., Su, G., Zheng, M., Gao, L., Liu, G., Liu, W., 2017. Degradation of one-side fully-chlorinated 1, 2, 3, 4-tetrachloronaphthalene over Fe–Al composite oxides and its hypothesized reaction mechanism. RSC Adv. 7 (29), 17577–17585.
Liu, Y., Meng, L., Han, K., Sun, S., 2021d. Synthesis of nano-zirconium-iron oxide supported by activated carbon composite for the removal of Sb (v) in aqueous solution. RSC Adv. 11 (49), 31131–31141.
Lu, J., Liu, D., Hao, J., Zhang, G., Lu, B., 2015. Phosphate removal from aqueous solutions by a nano-structured Fe–Ti bimetal oxide sorbent. Chem. Eng. Res. Des. 93, 652–661.
Lu, J., Wen, Z., Zhang, Y., Cheng, G., Xu, R., Gong, X., Wang, X., Chen, R., 2021. New insights on nanostructure of ordered mesoporous FeMn bimetal oxides (OMFMs) by a novel inverse micelle method and their superior arsenic sequestration performance: effect of calcination temperature and role of Fe/Mn oxides. Sci. Total Environ. 762, 143163.
Luo, J., Xuan, K., Wang, Y., Li, F., Wang, F., Pu, Y., Li, L., Zhao, N., Xiao, F., 2019. Aerobic oxidation of fluorene to fluorenone over Co–Cu bimetal oxides. New J. Chem. 43 (22), 8428–8438.
Mahar, A.M., Balouch, A., Talpur, F.N., Panah, P., Kumar, R., Kumar, A., Pato, A.H., Mal, D., Kumar, S., Umar, A.A., 2020. Fabrication of Pt-Pd@ ITO grown heterogeneous nanocatalyst as efficient remediator for toxic methyl parathion in aqueous media. Environ. Sci. Pollut. Res. 27 (9), 9970–9978.
Mansoori, S., Davarnejad, R., Ozumchelouei, E.J., Ismail, A.F., 2021. Activated biochar supported iron-copper oxide bimetallic catalyst for degradation of ciprofloxacin via photo-assisted electro-Fenton process: a mild pH condition. J. Water Process Eng. 39, 101888.
Mansour, S., Al-Wafi, R., Ahmed, M., Wageh, S., 2020. Microstructural, morphological behavior and removal of Cr (VI) and Se (IV) from aqueous solutions by magnetite nanoparticles/PVA and cellulose acetate nanofibers. Appl. Phys. A 126 (3), 1–14.
Markova, Z., Šišková, K.n.M., Filip, J., Čuda, J., Kolář, M., Šafářová, K.r., Medřík, I., Zbořil, R., 2013. Air stable magnetic bimetallic Fe–Ag nanoparticles for advanced antimicrobial treatment and phosphorus removal. Environ. Sci. Technol. 47 (10), 5285–5293.
Mehrabadi, B.A., Eskandari, S., Khan, U., White, R.D., Regalbuto, J.R., 2017. A review of preparation methods for supported metal catalysts. Adv. Catal. 61, 1–35.
Metwally, S., Rizk, H., 2014. Preparation and characterization of nano-sized iron–titanium mixed oxide for removal of some lanthanides from aqueous solution. Sep. Sci. Technol. 49 (15), 2426–2436.
Mirdamadi-Esfahani, M., Mostafavi, M., Keita, B., Nadjo, L., Kooyman, P., Remita, H., 2010. Bimetallic Au-Pt nanoparticles synthesized by radiolysis: application in electro-catalysis. Gold Bull. 43 (1), 49–56.
Mizukoshi, Y., Sato, K., Konno, T.J., Masahashi, N., 2010. Dependence of photocatalytic activities upon the structures of Au/Pd bimetallic nanoparticles immobilized on TiO2 surface. Appl. Catal. B 94 (3–4), 248–253.
Nagpal, V., Bokare, A.D., Chikate, R.C., Rode, C.V., Paknikar, K.M., 2010. Reductive dechlorination of γ-hexachlorocyclohexane using Fe–Pd bimetallic nanoparticles. J. Hazard. Mater. 175 (1–3), 680–687.
Nakarmi, A., Moreira, R., Bourdo, S.E., Watanabe, F., Toland, A., Viswanathan, T., 2020. Removal and recovery of phosphorus from contaminated water using novel, reusable, renewable resource-based aluminum/cerium oxide nanocomposite. Water Air Soil Pollut. 231 (12), 1–19.
Nehra, S., Dhillon, A., Kumar, D., 2020. Freeze–dried synthesized bifunctional biopolymer nanocomposite for efficient fluoride removal and antibacterial activity. J. Environ. Sci. 94, 52–63.
Nosrati, R., Olad, A., Nofouzi, K., 2015. A self-cleaning coating based on commercial grade polyacrylic latex modified by TiO2/Ag-exchanged-zeolite-A nanocomposite. Appl. Surf. Sci. 346, 543–553.
Ocsoy, I., Demirbas, A., McLamore, E.S., Altinsoy, B., Ildiz, N., Baldemir, A., 2017. Green synthesis with incorporated hydrothermal approaches for silver nanoparticles formation and enhanced antimicrobial activity against bacterial and fungal pathogens. J. Mol. Liq. 238, 263–269.
Organization, W.H., 2019. Water, sanitation, Hygiene and health: a Primer For Health Professionals. World Health Organization.
Organization, W.H., UNICEF., 2013. Progress on Sanitation and Drinking-Water. World Health Organization.
Padervand, M., Elahifard, M.R., Meidanshahi, R.V., Ghasemi, S., Haghighi, S., Gholami, M.R., 2012. Investigation of the antibacterial and photocatalytic properties of the zeolitic nanosized AgBr/TiO2 composites. Mater. Sci. Semicond. Process. 15 (1), 73–79.
Park, Y.M., Cho, J.M., Han, G.Y., Bae, J.W., 2021. Roles of highly ordered mesoporous structures of Fe–Ni bimetal oxides for an enhanced high-temperature water-gas shift reaction activity. Catal. Sci. Technol. 11 (9), 3251–3260.
Parvin, F., Rikta, S.Y., Tareq, S.M., 2019. Application of Nanomaterials For the Removal of Heavy Metal from wastewater, Nanotechnology in Water and Wastewater Treatment. Elsevier, pp. 137–157.
Pazhoor, M.T., Gautam, P.K., Samanta, S., Bangotra, P., Banerjee, S., 2021. Performance assessment of Zn–Sn bimetal oxides for the removal of inorganic arsenic in groundwater. Groundwater Sustain. Dev. 14, 100600.
Pereyra, A.M., Gonzalez, M.R., Rosato, V.G., Basaldella, E.I., 2014. A-type zeolite containing Ag+/Zn2+ as inorganic antifungal for waterborne coating formulations. Prog. Org. Coat. 77 (1), 213–218.
Polat, M., Soylu, A.M., Erdogan, D.A., Erguven, H., Vovk, E.I., Ozensoy, E., 2015. Influence of the sol–gel preparation method on the photocatalytic NO oxidation performance of TiO2/Al2O3 binary oxides. Catal. Today 241, 25–32.
Prabhu, S.M., Sasaki, K., Elanchezhiyan, S.S., Kalaignan, G.P., Park, C.M., 2020. Self-tuning tetragonal zirconia-based bimetallic nano (hydr) oxides as superior and recyclable adsorbents in arsenic-tolerant environment: template-free in and ex situ synthetic methods, stability, and mechanisms. Chem. Eng. J. 390, 124573.
Qin, J.-J., Oo, M.H., Kekre, K.A., 2007. Nanofiltration for recovering wastewater from a specific dyeing facility. Sep. Purif. Technol. 56 (2), 199–203.
Qu, X., Alvarez, P.J., Li, Q., 2013. Applications of nanotechnology in water and wastewater treatment. Water Res. 47 (12), 3931–3946.
Qu, X., Zhou, Y., Li, X., Javid, M., Huang, F., Zhang, X., Dong, X., Zhang, Z., 2020. Nitrogen-doped graphene layer-encapsulated NiFe bimetallic nanoparticles synthesized by an arc discharge method for a highly efficient microwave absorber. Inorg. Chem. Front. 7 (5), 1148–1160.
Quinson, J., Jensen, K.M., 2020. From platinum atoms in molecules to colloidal nanoparticles: a review on reduction, nucleation and growth mechanisms. Adv. Colloid Interface Sci., 102300.
Raghav, S., Nair, M., Kumar, D., 2019. Tetragonal prism shaped Ni-Al bimetallic adsorbent for study of adsorptive removal of fluoride and role of ion-exchange. Appl. Surf. Sci. 498, 143785.
Rahaghi, S.H., Poursalehi, R., Miresmaeili, R., 2015. Optical properties of Ag-Cu alloy nanoparticles synthesized by DC arc discharge in liquid. Procedia Mater. Sci. 11, 738–742.
Rahimi, M., Pourmortazavi, S.M., Zandavar, H., Mirsadeghi, S., 2021. Recyclable methodology over bimetallic zero-valent Mg: Zn composition for hexavalent chromium reme-

diation via batch and flow systems in industrial wastewater: an experimental design. J. Mater. Res. Technol. 11, 1–18.
Rana, S., Jonnalagadda, S.B., 2017. A facile synthesis of Cu–Ni bimetallic nanoparticle supported organo functionalized graphene oxide as a catalyst for selective hydrogenation of p-nitrophenol and cinnamaldehyde. RSC Adv. 7 (5), 2869–2879.
Rashid, S., Shen, C., Chen, X., Li, S., Chen, Y., Wen, Y., Liu, J., 2015. Enhanced catalytic ability of chitosan–Cu–Fe bimetal complex for the removal of dyes in aqueous solution. RSC Adv. 5 (110), 90731–90741.
Rocheleau, R.E., Zhang, Z., Gilje, J.W., Meese-Marktscheffel, J.A., 1994. MOCVD deposition of MgAl2O4 films using metal alkoxide precursors. Chem. Mater. 6 (10), 1615–1619.
Sankar, M., Dimitratos, N., Miedziak, P.J., Wells, P.P., Kiely, C.J., Hutchings, G.J., 2012. Designing bimetallic catalysts for a green and sustainable future. Chem. Soc. Rev. 41 (24), 8099–8139.
Savage, N., Diallo, M.S., 2005. Nanomaterials and water purification: opportunities and challenges. J. Nanopart. Res. 7 (4), 331–342.
Scaria, J., Nidheesh, P., Kumar, M.S., 2020. Synthesis and applications of various bimetallic nanomaterials in water and wastewater treatment. J. Environ. Manage. 259, 110011.
Schellenberg, T., Subramanian, V., Ganeshan, G., Tompkins, D., Pradeep, R., 2020. Wastewater discharge standards in the evolving context of urban sustainability–The case of India. Front. Environ. Sci. 8, 30.
Sharma, G., Kumar, A., Sharma, S., Naushad, M., Dwivedi, R.P., ALOthman, Z.A., Mola, G.T., 2019a. Novel development of nanoparticles to bimetallic nanoparticles and their composites: a review. J. King Saud Univ.-Sci. 31 (2), 257–269.
Sharma, R.K., Arora, B., Sharma, S., Dutta, S., Sharma, A., Yadav, S., Solanki, K., 2020. In situ hydroxyl radical generation using the synergism of the Co–Ni bimetallic centres of a developed nanocatalyst with potent efficiency for degrading toxic water pollutants. Mater. Chem. Front. 4 (2), 605–620.
Sharma, V.K., Sohn, M., McDonald, T.J., 2019b. Remediation of selenium in water: a review. In: Advances in Water Purification Techniques, pp. 203–218.
Shu, Z., Zhang, Y., Yang, Q., Yang, H., 2017. Halloysite nanotubes supported Ag and ZnO nanoparticles with synergistically enhanced antibacterial activity. Nanoscale Res. Lett. 12 (1), 1–7.
Singh, H.P., Gupta, N., Sharma, S.K., Sharma, R.K., 2013. Synthesis of bimetallic Pt–Cu nanoparticles and their application in the reduction of rhodamine B. Colloids Surf. A 416, 43–50.
Singh, S., Joshi, H.C., Srivastava, A., Sharma, A., Verma, N., 2014. An efficient antibacterial multi-scale web of carbon fibers with asymmetrically dispersed Ag–Cu bimetal nanoparticles. Colloids Surf. A 443, 311–319.
Sivasankar, V., Nkonde, M.A., Govender, P., Omine, K., Kuvarega, A.T., Prabhakaran, M., Msagati, T.A., 2018. Dendrimer supported Fe/Ni bimetallic composites immobilized in polyethersulfone membranes for effective degradation of arginine containing microcystins. Eur. Polym. J. 98, 456–467.
Song, D., Li, T., Wei, Y.-Y., Xu, .Z..-R., 2020. Controlled formation of porous CuCo2O4 nanorods with enhanced oxidase and catalase catalytic activities using bimetal-organic frameworks as templates. Colloids Surf. B 188, 110764.
Song, J., Huang, G., Han, D., Hou, Q., Gan, L., Zhang, M., 2021. A review of reactive media within permeable reactive barriers for the removal of heavy metal (loid) s in groundwater: current status and future prospects. J. Clean. Prod., 128644.
Song, S., Zhang, S., Huang, S., Zhang, R., Yin, L., Hu, Y., Wen, T., Zhuang, L., Hu, B., Wang, X., 2019. A novel multi-shelled Fe3O4@ MnOx hollow microspheres for immobilizing U (VI) and Eu (III). Chem. Eng. J. 355, 697–709.
Sui, H., Rong, Y., Song, J., Zhang, D., Li, H., Wu, P., Shen, Y., Huang, Y., 2018. Mechanochemical destruction of DDTs with Fe-Zn bimetal in a high-energy planetary ball mill. J. Hazard. Mater. 342, 201–209.
Sun, M., Zeng, Z., Peng, L., Han, Z., Yu, C., Cheng, S., Xie, J., 2021. Ultrathin polymer electrolyte film prepared by in situ polymerization for lithium metal batteries. Mater. Today Energy 21, 100785.
Taha, M.A., Youness, R.A., Zawrah, M.F., 2019. Review on nanocomposites fabricated by mechanical alloying. Int. J. Miner. Metall. Mater. 26 (9), 1047–1058.
Tao, G., Hua, Z., Gao, Z., Zhu, Y., Chen, Y., Shu, Z., Zhang, L., Shi, J., 2013. KF-loaded mesoporous Mg–Fe bi-metal oxides: high performance transesterification catalysts for biodiesel production. Chem. Commun. 49 (73), 8006–8008.
Taoufik, N., Boumya, W., Achak, M., Sillanpää, M., Barka, N., 2021. Comparative overview of advanced oxidation processes and biological approaches for the removal pharmaceuticals. J. Environ. Manage. 288, 112404.
Tee, Y.-H., Grulke, E., Bhattacharyya, D., 2005. Role of Ni/Fe nanoparticle composition on the degradation of trichloroethylene from water. Ind. Eng. Chem. Res. 44 (18), 7062–7070.
Tian, H., Li, J., Mu, Z., Li, L., Hao, Z., 2009. Effect of pH on DDT degradation in aqueous solution using bimetallic Ni/Fe nanoparticles. Sep. Purif. Technol. 66 (1), 84–89.
Tian, N., Zhou, Z., Tian, X., Yang, C., Li, Y., 2017. Superior capability of MgAl2O4 for selenite removal from contaminated groundwater during its reconstruction of layered double hydroxides. Sep. Purif. Technol. 176, 66–72.
Tian, Y., He, X., Zhou, H., Tian, X., Nie, Y., Zhou, Z., Yang, C., Li, Y., 2020. Efficient fenton-like degradation of ofloxacin over bimetallic Fe–Cu@ Sepiolite composite. Chemosphere 257, 127209.
Tkaczyk, A., Mitrowska, K., Posyniak, A., 2020. Synthetic organic dyes as contaminants of the aquatic environment and their implications for ecosystems: a review. Sci. Total Environ. 717, 137222.
Todorovska, R., Groudeva-Zotova, S., Todorovsky, D., Tzvetkov, G., Stefanov, P., 2002. Highly Crystalline Y3Fe5O12 Thin Films by Cictric Spray Pyrolysis. J. Mater. Synth. Process. 10 (5), 283–288.
Urase, T., Kikuta, T., 2005. Separate estimation of adsorption and degradation of pharmaceutical substances and estrogens in the activated sludge process. Water Res. 39 (7), 1289–1300.
Veith, M., Haas, M., Huch, V., 2005. Single source precursor approach for the sol– gel synthesis of nanocrystalline ZnFe2O4 and zinc– iron oxide composites. Chem. Mater. 17 (1), 95–101.
Vieno, N., Tuhkanen, T., Kronberg, L., 2006. Removal of pharmaceuticals in drinking water treatment: effect of chemical coagulation. Environ. Technol. 27 (2), 183–192.
Vilardi, G., 2020. P-aminophenol catalysed production on supported nano-magnetite particles in fixed-bed reactor: kinetic modelling and scale-up. Chemosphere 250, 126237.
Vilardi, G., Parisi, M., Verdone, N., 2019a. Simultaneous aggregation and oxidation of nZVI in Rushton equipped agitated vessel: experimental and modelling. Powder Technol. 353, 238–246.
Vilardi, G., Stoller, M., Di Palma, L., Boodhoo, K., Verdone, N., 2019b. Metallic iron nanoparticles intensified production by spinning disk reactor: optimization and fluid dynamics modelling. Chem. Eng. Process.-Process Intensif. 146, 107683.
Vilardi, G., Verdone, N., 2020. Production of metallic iron nanoparticles in a baffled stirred tank reactor: optimization via computational fluid dynamics simulation. Particuology 52, 83–96.
Vilardi, G., Verdone, N., Bubbico, R., 2021. Combined production of metallic-iron nanoparticles: exergy and energy analysis of two alternative processes using Hydrazine and NaBH4 as reducing agents. J. Taiwan Inst. Chem. Eng. 118, 97–111.
Wadhawan, S., Jain, A., Nayyar, J., Mehta, S.K., 2020. Role of nanomaterials as adsorbents in heavy metal ion removal from waste water: a review. J. Water Process Eng. 33, 101038.
Walha, K., Amar, R.B., Firdaous, L., Quéméneur, F., Jaouen, P., 2007. Brackish groundwater treatment by nanofiltration, reverse osmosis and electrodialysis in Tunisia: performance and cost comparison. Desalination 207 (1–3), 95–106.
Wan, Y., Zhao, W., Tang, Y., Li, L., Wang, H., Cui, Y., Gu, J., Li, Y., Shi, J., 2014. Ni-Mn bi-metal oxide catalysts for the low temperature SCR removal of NO with NH3. Appl. Catal. B 148, 114–122.
Wang, J., Wang, B., Liu, Z., Fan, L., Zhang, Q., Ding, H., Wang, L., Yang, H., Yu, X., Lu, B., 2019. Nature of bimetallic oxide Sb2MoO6/rGO anode for high-performance potassium-ion batteries. Adv. Sci. 6 (17), 1900904.
Wang, R., Tang, T., Lu, G., Huang, K., Yin, H., Lin, Z., Wu, F., Dang, Z., 2018. Rapid debromination of polybrominated diphenyl ethers (PBDEs) by zero valent metal and bimetals: mechanisms and pathways assisted by density function theory calculation. Environ. Pollut. 240, 745–753.
Wang, T., Jiao, Y., He, M., Ouyang, W., Lin, C., Liu, X., 2022. Facile co-removal of As (V) and Sb (V) from aqueous solution using Fe-Cu binary oxides: structural modification and self-driven force field of copper oxides. Sci. Total Environ. 803, 150084.
Wang, X., Chen, C., Chang, Y., Liu, H., 2009. Dechlorination of chlorinated methanes by Pd/Fe bimetallic nanoparticles. J. Hazard. Mater. 161 (2–3), 815–823.
Wang, Y., Chen, J., Guan, M., Qiu, H., 2021. Preparation of Fe/Ni bimetallic oxide porous graphene composite materials for efficient adsorption and removal of sulfonamides. Langmuir.
Wangcheng, Z., ZHANG, X., Yanglong, G., Li, W., Yun, G., Guanzhong, L., 2014. Synthesis of mesoporous CeO2-MnOx binary oxides and their catalytic performances for CO oxidation. J. Rare Earths 32 (2), 146–152.
Wen, Z., Lu, J., Zhang, Y., Cheng, G., Huang, S., Chen, J., Xu, R., Ming, Y.-a., Wang, Y., Chen, R., 2020. Facile inverse micelle fabrication of magnetic ordered mesoporous iron cerium bimetal oxides with excellent performance for arsenic removal from water. J. Hazard. Mater. 383, 121172.
Wen, Z., Zhang, Y., Cheng, G., Wang, Y., Chen, R., 2019. Simultaneous removal of As (V)/Cr (VI) and acid orange 7 (AO7) by nanosized ordered magnetic mesoporous Fe-Ce bimetal oxides: behavior and mechanism. Chemosphere 218, 1002–1013.
Weng, X., Cai, W., Lan, R., Sun, Q., Chen, Z., 2018. Simultaneous removal of amoxicillin, ampicillin and penicillin by clay supported Fe/Ni bimetallic nanoparticles. Environ. Pollut. 236, 562–569.
Wu, T.-S., Wang, K.-X., Li, G.-D., Sun, S.-Y., Sun, J., Chen, .J..-S., 2010. Montmorillonite–supported Ag/TiO2 nanoparticles: an efficient visible-light bacteria photodegradation material. ACS Appl. Mater. Interfaces 2 (2), 544–550.
Xie, W., Liang, Q., Qian, T., Zhao, D., 2015. Immobilization of selenite in soil and groundwater using stabilized Fe–Mn binary oxide nanoparticles. Water Res. 70, 485–494.
Xie, X., Lu, C., Xu, R., Yang, X., Yan, L., Su, C., 2022. Arsenic removal by manganese-doped mesoporous iron oxides from groundwater: performance and mechanism. Sci. Total Environ. 806, 150615.
Xie, Y., Chen, C., Lu, X., Luo, F., Wang, C., Alsaedi, A., Hayat, T., 2019. Porous NiFe-oxide nanocubes derived from prussian blue analogue as efficient adsorbents for the removal of toxic metal ions and organic dyes. J. Hazard. Mater. 379, 120786.
Xie, Y., Fang, Z., Cheng, W., Tsang, P.E., Zhao, D., 2014. Remediation of polybrominated diphenyl ethers in soil using Ni/Fe bimetallic nanoparticles: influencing factors, kinetics and mechanism. Sci. Total Environ. 485, 363–370.
Xu, R., Xie, Y., Tian, J., Chen, L., 2021a. Adsorbable organic halogens in contaminated water environment: a review of sources and removal technologies. J Clean Prod 283, 124645.
Xu, Y., Hu, E., Xu, D., Guo, Q., 2021b. Activation of peroxymonosulfate by bimetallic CoMn oxides loaded on coal fly ash-derived SBA-15 for efficient degradation of Rhodamine B. Sep. Purif. Technol., 119081.
Yan, S., Zhou, K., Li, Y., He, Q., Xia, L., Liu, S., Li, H., Liang, D., Song, S., 2020. Efficient removal of As (V) from diluted aqueous solutions by Fe/La oxide magnetic microspheres. J. Clean. Prod. 273, 123134.
Yanan, S., Xing, X., Yue, Q., Gao, B., Li, Y., 2020. Nitrogen-doped carbon nanotubes encapsulating Fe/Zn nanoparticles as a persulfate activator for sulfamethoxazole degradation: role of encapsulated bimetallic nanoparticles and nonradical reaction. Environ. Sci. 7 (5), 1444–1453.

Yang, K., Li, C., Wang, X., Liu, Y., Li, Y., Zhou, C., Wang, Z., Zhou, J., Cao, Z., Xu, X., 2020a. Functional adjustment and cyclic application of Fe–Mn bimetal composite for Sb (V) removal: transformation of iron oxides forms and a stable regeneration method. J. Clean. Prod. 266, 122007.

Yang, X., Cai, J., Wang, X., Li, Y., Wu, Z., Wu, W.D., Chen, X.D., Sun, J., Sun, S.-P., Wang, Z., 2020b. A bimetallic Fe–Mn oxide-activated oxone for in situ chemical oxidation (ISCO) of trichloroethylene in groundwater: efficiency, sustained activity, and mechanism investigation. Environ. Sci. Technol. 54 (6), 3714–3724.

Yang, Y., Xu, L., Wang, J., 2021. An enhancement of singlet oxygen generation from dissolved oxygen activated by three-dimensional graphene wrapped nZVI-doped amorphous Al species for chloramphenicol removal in the Fenton-like system. Chem. Eng. J. 425, 131497.

Ye, J., Wang, Y., Xu, Q., Wu, H., Tong, J., Shi, J., 2021. Removal of hexavalent chromium from wastewater by Cu/Fe bimetallic nanoparticles. Sci. Rep. 11 (1), 1–11.

Yin, H., Li, J., Yan, H., Cai, H., Wan, Y., Yao, G., Guo, Y., Lai, B., 2021. Activation of peroxymonosulfate by CuCo2O4 nano-particles towards long-lasting removal of atrazine. J. Water Reuse Desalin..

Yu, H., He, Y., 2015. Seed-assisted synthesis of dendritic Au–Ag bimetallic nanoparticles with chemiluminescence activity and their application in glucose detection. Sens. Actuat. B 209, 877–882.

Yu, Y., Chen, J.P., 2014. Fabrication and performance of a Mn–La metal composite for remarkable decontamination of fluoride. J. Mater. Chem. A 2 (21), 8086–8093.

Yuan, X., Dragoe, D., Beaunier, P., Uribe, D.B., Ramos, L., Méndez-Medrano, M.G., Remita, H., 2020. Polypyrrole nanostructures modified with mono-and bimetallic nanoparticles for photocatalytic H 2 generation. J. Mater. Chem. A 8 (1), 268–277.

Zhang, D., Li, Y., Guo, J., Zhou, L., Lan, Y., Chen, C., 2021a. MOFs-derived magnetic C@ Cu–Ni bimetal particles: an efficient peroxymonosulfate activator for 2, 4, 6-trichlorophenol degradation. Chemosphere 269, 129394.

Zhang, J., Zhang, L., Jia, Y., Chen, G., Wang, X., Kuang, Q., Xie, Z., Zheng, L., 2012. Synthesis of spatially uniform metal alloys nanocrystals via a diffusion controlled growth strategy: the case of Au-Pd alloy trisoctahedral nanocrystals with tunable composition. Nano Res. 5 (9), 618–629.

Zhang, Q., Sun, X., Dang, Y., Zhu, J.-J., Zhao, Y., Xu, X., Zhou, Y., 2021b. A novel electrochemically enhanced homogeneous PMS-heterogeneous CoFe2O4 synergistic catalysis for the efficient removal of levofloxacin. J. Hazard. Mater., 127651.

Zhang, Z., Hu, Y.-b., Ruan, W., Ai, H., Yuan, B., Fu, .M..-L., 2021c. Highly improved dechlorination of 2, 4-dichlorophenol in aqueous solution by Fe/Ni nanoparticles supported by polystyrene resin. Chemosphere 266, 128976.

Zhang, Z., Shen, Q., Cissoko, N., Wo, J., Xu, X., 2010. Catalytic dechlorination of 2, 4-dichlorophenol by Pd/Fe bimetallic nanoparticles in the presence of humic acid. J. Hazard. Mater. 182 (1–3), 252–258.

Zhao, L., Huang, Y., Chen, H., Zhao, Y., Xiao, T., 2017. Study on the preparation of bimetallic oxide sorbent for mercury removal. Fuel 197, 20–27.

Zheng, Z., Yuan, S., Liu, Y., Lu, X., Wan, J., Wu, X., Chen, J., 2009. Reductive dechlorination of hexachlorobenzene by Cu/Fe bimetal in the presence of nonionic surfactant. J. Hazard. Mater. 170 (2–3), 895–901.

Zhong, X., Lu, Z., Liang, W., Hu, B., 2021. Incorporating bimetal oxide MnFe2O4 onto covalent organic frameworks for the removal of UO22+ ion from aqueous solution. Appl. Surf. Sci. 556, 149581.

Zhu, N., Luan, H., Yuan, S., Chen, J., Wu, X., Wang, L., 2010. Effective dechlorination of HCB by nanoscale Cu/Fe particles. J. Hazard. Mater. 176 (1–3), 1101–1105.